

## **Investigating the effect of Target of Rapamycin kinase inhibition on the *Chlamydomonas reinhardtii* phosphoproteome: from known homologs to new targets**

Emily G. Werth<sup>1</sup>, Evan W. McConnell<sup>1</sup>, Inmaculada Couso<sup>2,3</sup>, Zoe Perrine<sup>2</sup>, Jose L. Crespo<sup>3</sup>, James G. Umen<sup>2</sup>, and Leslie M. Hicks<sup>1</sup>

<sup>1</sup>Department of Chemistry, University of North Carolina at Chapel Hill, Chapel Hill, NC

<sup>2</sup>Donald Danforth Plant Science Center, St. Louis, MO 63132, USA

<sup>3</sup> Instituto de Bioquímica Vegetal y Fotosíntesis, Consejo Superior de Investigaciones Científicas (CSIC)—Universidad de Sevilla; Avda. Américo Vespucio, 49, 41092 Sevilla, Spain

**Correspondence:** Dr. Leslie M. Hicks, Department of Chemistry, University of North Carolina at Chapel Hill, 125 South Road, CB#3290, Chapel Hill, NC 27599

**E-mail:** [lmhicks@unc.edu](mailto:lmhicks@unc.edu)

**Phone/Fax:** 1-919-843-6903/919-962-2388

Total word count: 5361

Introduction: 736

Materials and Methods: 1613

Results: 1372

Discussion: 1594

Acknowledgements: 46

Number of Tables: 2

Number of Figures: 6, 5 in color

Number of Supplemental Tables: 5

Number of Supplemental Figures: 4

## 1 Summary

- 2 • Target of Rapamycin (TOR) kinase is a conserved regulator of cell growth whose activity is  
3 modulated in response to nutrients, energy and stress. Key proteins involved in the pathway  
4 are conserved in the model photosynthetic microalga *Chlamydomonas reinhardtii*, but the  
5 substrates of TOR kinase and downstream signaling network have not been elucidated. Our  
6 study provides a new resource for investigating the phosphorylation networks governed by the  
7 TOR kinase pathway in *Chlamydomonas*.
- 8 • We used quantitative phosphoproteomics to investigate the effects of inhibiting  
9 *Chlamydomonas* TOR kinase on dynamic protein phosphorylation. Wild-type and AZD-  
10 insensitive *Chlamydomonas* strains were treated with TOR-specific chemical inhibitors  
11 (rapamycin, AZD8055 and Torin1), after which differentially affected phosphosites were  
12 identified.
- 13 • Our quantitative phosphoproteomic dataset comprised 2,547 unique phosphosites from 1,432  
14 different proteins. Inhibition of TOR kinase caused significant quantitative changes in  
15 phosphorylation at 258 phosphosites, from 219 unique phosphopeptides.
- 16 • Our results include *Chlamydomonas* homologs of TOR signaling-related proteins, including a  
17 site on RPS6 with a decrease in phosphorylation. Additionally, phosphosites on proteins  
18 involved in translation and carotenoid biosynthesis were identified. Follow-up experiments  
19 guided by these phosphoproteomic findings in lycopene beta/epsilon cyclase showed that  
20 carotenoid levels are affected by TORC1 inhibition and carotenoid production is under TOR  
21 control in algae.

22 Keywords: Phosphoproteomics, *Chlamydomonas*, AZD8055, rapamycin, Torin1, target of  
23 rapamycin, TOR, NL

## 24 **Introduction**

25 The Target of Rapamycin (TOR) protein kinase is a conserved eukaryotic growth regulator whose  
26 activity is modulated in response to stress, nutrients and energy supply (Wullschleger *et al.*, 2006;  
27 Loewith & Hall, 2011; Dobrenel *et al.*, 2016a; González & Hall, 2017; Pérez-Pérez *et al.*, 2017).  
28 In metazoans and fungi, TOR is found in two compositionally and functionally distinct  
29 multiprotein complexes (TORC1) and (TORC2) that control rates of biosynthetic growth and  
30 cytoskeletal dynamics respectively (Raught *et al.*, 2001; Wullschleger *et al.*, 2006). In the green  
31 lineage (algae and land plants), only homologs of TORC1 proteins have been identified (Diaz-  
32 Troya *et al.*, 2008; van Dam *et al.*, 2011; Dobrenel *et al.*, 2016a). TORC1 kinase activity is  
33 modulated by nutrients and stress, and serves to control protein biosynthesis and other metabolic  
34 processes in response to environmental conditions (Raught *et al.*, 2001). Selective chemical  
35 inhibitors of TOR kinase including rapamycin, AZD8055, and Torin1 have been instrumental in  
36 dissecting the TOR signaling pathway (Fingar & Blenis, 2004; Thoreen *et al.*, 2009; Chresta *et al.*,  
37 2010; Benjamin *et al.*, 2011). Rapamycin (Rap) inhibits TORC1 activity through an allosteric  
38 mechanism requiring formation of a FKBP12-Rap complex (Heitman *et al.*, 1991; Brown *et al.*,  
39 1994; Sabatini *et al.*, 1994). Recent studies support the notion that several functions of TOR kinase  
40 are not inhibited by rapamycin (Thoreen *et al.*, 2009). Instead, novel drugs like Torin1 and  
41 AZD8055 have been reported to more completely inhibit TOR kinase by acting as ATP-  
42 competitors (Thoreen *et al.*, 2009; Chresta *et al.*, 2010). Torin1 has slower off-binding kinetics  
43 than other mTOR inhibitors in mammalian cell lines, possibly due to conformational change  
44 induction in the kinase that is energetically more difficult to recover from leading to a more  
45 pronounced and longer inhibition of the TORC1 pathway (Liu *et al.*, 2013). AZD8055 is an ATP-  
46 competitive inhibitor of mTOR and all PI3K class I isoforms noted to inhibit the mTORC1 and  
47 mTORC2 substrate phosphorylation (Roohi & Hojjat-Farsangi, 2017). These drugs were used to  
48 inhibit TOR activity in plants where rapamycin treatment is not highly effective (Zhang *et al.*,  
49 2011; Montane & Menand, 2013).

50 The role of TOR in mammalian and fungal cell metabolism has been extensively investigated  
51 (Wullschleger *et al.*, 2006; Dibble & Manning, 2013; Saxton & Sabatini, 2017), while its role in  
52 photosynthetic eukaryotes is less well established (Zhang *et al.*, 2013; Xiong & Sheen, 2014;  
53 Dobrenel *et al.*, 2016a). TOR has been shown to control growth, metabolism and life span in the

54 model plant *Arabidopsis thaliana* (*Arabidopsis*) (Dobrenel *et al.*, 2011; Ren *et al.*, 2012; Xiong,  
55 Y. & Sheen, J., 2012; Xiong *et al.*, 2013) where the TOR gene is essential (Menand *et al.*, 2002).  
56 The model green alga *Chlamydomonas reinhardtii* (*Chlamydomonas*) has key TORC1 complex  
57 proteins encoded by single-copy genes including TOR (Cre09.g400553.t1.1), regulatory associate  
58 protein target of rapamycin (RAPTOR) (Cre08.g371957.t1.1), and lethal with sec-13 protein 8  
59 (LST8) (Cre17.g713900.t1.2) (Diaz-Troya *et al.*, 2008; van Dam *et al.*, 2011). Treatment of  
60 *Chlamydomonas* cultures with rapamycin has been shown to slow but not completely arrest cell  
61 growth (Crespo *et al.*, 2005), activate autophagy (Perez-Perez *et al.*, 2010), and induce lipid droplet  
62 formation (Imamura *et al.*, 2015; Rodrigues *et al.*, 2015). Recent work reported a connection  
63 between TOR kinase and inositol polyphosphate signaling that governs carbon metabolism and  
64 lipid accumulation (Couso *et al.*, 2016). *Chlamydomonas* cells are sensitive to Torin1 and  
65 AZD8055 that are potent inhibitors of cell growth at saturating doses (Couso *et al.*, 2016) and  
66 induce triacylglycerol accumulation (Imamura *et al.*, 2016). However, the TOR pathway in  
67 *Chlamydomonas* has yet to be extensively characterized and, to date, only a limited number of  
68 candidate TOR kinase substrates have been identified.

69 We characterized the phosphoproteome of *Chlamydomonas* that produced a conservative estimate  
70 of 4,588 phosphoproteins / 15,862 unique phosphosites (Wang *et al.*, 2014) through a qualitative  
71 strategy involving extensive fractionation and complementary enrichment strategies, and have  
72 now developed label-free quantification (LFQ) to allow simultaneous quantification of 2,547  
73 *Chlamydomonas* phosphosites (Werth *et al.*, 2017). Herein we characterized the effects of TOR  
74 inhibition on the *Chlamydomonas* phosphoproteome. Cultures treated with saturating doses of  
75 different TOR inhibitors (rapamycin, AZD8055 and Torin1) revealed hundreds of affected  
76 phosphosites with a significant overlap observed between those seen with different inhibitors.  
77 Phosphosites from an AZD-resistant mutant were compared with wild type after AZD treatment  
78 revealing very few potential off target effects. Hierarchical clustering was used to classify sites  
79 and motif analysis was used to assess consensus motifs in clusters.

## 80 **Materials and Methods**

### 81 *Cell culturing and drug treatment.*

82 Strain CC-1690 wild-type mt<sup>+</sup> (Sager 21 gr) (Sager, 1955) was used for the wild-type  
83 Chlamydomonas analysis across all chemical inhibitors. For the control AZD-insensitive strain  
84 experiments, strain was obtained from the Umen laboratory (Donald Danforth Plant Science  
85 Center). All cultures were maintained on TAP (Tris acetate phosphate) agar plates and grown in  
86 350-mL TAP liquid cultures at 25°C as previously described (Couso *et al.*, 2016). Experiments  
87 were done using five replicate cultures grown to exponential phase ( $1-2 \times 10^6$  cells/mL) for each  
88 drug condition and control and quenched with 40% methanol prior to harvesting by centrifuging  
89 at 4000 g for 5 min and discarding supernatant. To limit batch effects, replicate “n” of each drug  
90 and control were harvested together (Figure 1) prior to downstream processing. Cell pellets were  
91 then flash frozen using liquid nitrogen and stored at -80°C until use. For AZD8055-, Torin 1-, and  
92 rapamycin- treated (LC Laboratories) cultures, drug was added to a final concentration of 500 nM  
93 for rapamycin and Torin 1, and 700 nM for AZD8055 from 1mM stocks in DMSO for 15 min  
94 prior to harvesting. For control replicates, just drug vehicle (DMSO) without a chemical inhibitor  
95 was added to each replicate culture for 15 min prior to harvesting.

### 96 *Protein extraction.*

97 Cell pellets were resuspended in lysis buffer containing 100 mM Tris, pH 8.0 with 1x  
98 concentrations of cOmplete protease inhibitor and phosSTOP phosphatase inhibitor cocktails  
99 (Roche, Indianapolis, IN, USA). Cells were lysed via sonication using an E220 focused  
100 ultrasonicator (Covaris, Woburn, MA, USA) for 120 s at 200 cycles/burst, 100 W power and 13%  
101 duty cycle. Following ultrasonication, the supernatant was collected from cellular debris by  
102 centrifugation for 10 min at 15,000 g at 4°C and proteins were precipitated using 5 volumes of  
103 cold 100 mM ammonium acetate in methanol. Following 3 hr incubation at -80°C, protein was  
104 pelleted by centrifugation for 5 min at 2,000 g followed by two washes with fresh 100 mM  
105 ammonium acetate in methanol and a final wash with 70% ethanol. Cell pellets were resuspended  
106 in 8M urea and protein concentration was determined using the CB-X assay (G-Biosciences, St.  
107 Louis, MO, USA).

108

109 *Protein digestion and reduction.*

110 Samples were reduced using 10 mM dithiothreitol for 30 min at RT and subsequently alkylated  
111 with 40 mM iodoacetamide for 45 min in darkness at RT prior to overnight digestion. Samples  
112 were diluted 5-fold in 100 mM Tris following alkylation and digestion was performed at 25C for  
113 16 h with Trypsin Gold (Promega) at a protease:protein ratio of 1:50.

114 *Solid-phase extraction.*

115 After digestion, samples were acidified to pH<3.0 with trifluoroacetic acid (TFA). Pelleted,  
116 undigested protein was cleared from the supernatant by centrifugation for 5 min at 5,000 g prior  
117 to solid-phase extraction. Desalting was performed using C18 50 mg Sep-Pak cartridges (Waters).  
118 Columns were prepared by washing with acetonitrile (MeCN) followed by 80%  
119 MeCN/20% $H_2O$ /0.1% TFA and 0.1% TFA. Digested protein lysates were applied to the columns  
120 and reloaded twice before being washed with 0.1% TFA and eluted using 80%  
121 MeCN/20% $H_2O$ /0.1% TFA.

122 *Phosphopeptide enrichment and clean-up.*

123 Following protein digestion and solid-phase extraction, replicates were dried down using vacuum  
124 centrifugation and phosphopeptide enrichment was performed on 2-mg aliquots of each sample  
125 using 3 mg Titansphere Phos- $TiO_2$  kit spin columns (GL Sciences) as previously described (Werth  
126 *et al.*, 2017). After enrichment, samples were dried down and desalted again using ZipTips  
127 (Millipore) as per manufacturers protocol prior to LC-MS/MS acquisition.

128 *LC-MS/MS acquisition and data processing.*

129 Following ZipTip clean-up, peptides were dried down and resuspended in 20  $\mu$ L of 0.1% TFA,  
130 5% MeCN before separation via a 90-min linear gradient from 95%  $H_2O$ /5% MeCN/0.1% formic  
131 acid (FA) to 65%  $H_2O$ /35% MeCN/0.1% FA via a NanoAcquity UPLC (Waters) using a C18  
132 column (NanoAcquity UPLC 1.8  $\mu$ m HSS T3, 75  $\mu$ m  $\times$  250 mm). A TripleTOF 5600 (AB Sciex)  
133 Q-TOF was operated in positive-ionization nanoelectrospray and high-sensitivity mode for data  
134 acquisition as previously described (Slade *et al.*, 2015). In addition to the Supporting Information  
135 tables for MS datasets, the mass spectrometry proteomics data have been deposited to the  
136 ProteomeXChange Consortium via PRIDE partner repository(Vizcaíno *et al.*, 2013) identifier

137 PXD007221. Acquired spectra (\*.wiff) files were imported into Progenesis QI for proteomics  
138 (v2.0, Nonlinear Dynamics) as previously described (Werth *et al.*, 2017) with peptide sequence  
139 determination and protein inference done by Mascot (v.2.5.1; Matrix Science) using the *C.*  
140 *reinhardtii* Phytozome v.11 database ([www.phytozome.net/](http://www.phytozome.net/); accessed May 2015) appended with  
141 the NCBI chloroplast and mitochondrial databases (19,603 entries) and sequences for common  
142 laboratory contaminants (<http://thegpm.org/cRAP/>; 116 entries). For database searching, trypsin  
143 protease specificity with up to two missed cleavages, peptide/fragment mass tolerances of 20  
144 ppm/0.1 Da, a fixed modification of carbamidomethylation at cysteine, and variable modifications  
145 of acetylation at the protein N-terminus, oxidation at methionine, deamidation at asparagine or  
146 glutamine, phosphorylation at serine or threonine and phosphorylation at tyrosine were used.  
147 Peptide false discovery rates (FDR) were adjusted to  $\leq 1\%$  using the Mascot Percolator algorithm  
148 (Käll *et al.*, 2007) and only peptides with a Mascot ion score over 13 were considered.

149 Custom scripts written in Python were implemented to parse results following data normalization  
150 and quantification in Progenesis QI for proteomics. Shared peptides between proteins were  
151 grouped together to satisfy the principle of parsimony and represented in Table S1 by the protein  
152 accession with the highest amount of unique peptides, otherwise the largest confidence score  
153 assigned by Progenesis QI for proteomics. Additionally, the script appended site localization of  
154 variable modifications using an implementation of the Mascot Delta Score (Savitski *et al.*, 2011)  
155 to the peptide measurements (\*.csv) export from Progenesis QI for proteomics with confident site  
156 localization considered a Mascot Delta score  $>90\%$ . Following scoring, only peptides with  
157 phosphorylation at serine, threonine, or tyrosine were considered for further processing and  
158 analysis.

#### 159 *Downstream bioinformatics analysis.*

160 Missing value imputation was performed on logarithmized normalized abundances in Perseus  
161 v1.6.0.0 (Cox & Mann, 2012; Tyanova *et al.*, 2016) requiring at least three of the five replicates  
162 in all drug conditions and control to be nonzero to continue through the workflow. A coefficient  
163 of variation (CV) cutoff was applied requiring  $CV < 25\%$  in at least 2 of 4 conditions for each  
164 phosphosite. For t-test analyses, replicates were grouped and the statistical tests were performed  
165 with fold change threshold of  $\pm 2$  and  $p \leq 0.05$  significance threshold. KEGG pathway annotation  
166 (Kanehisa & Goto, 2000), Gene Ontology (GO) (Ashburner *et al.*, 2000) term annotation,

167 hierarchical clustering, and motif analysis were performed following statistical testing to glean  
168 biological insight on modulated sites found in the study. For hierarchical clustering, visualization  
169 was performed in Perseus v1.6.0.0. Following data normalization and missing value imputation,  
170 intensity values were z-score normalized and grouped using k-means clustering with default  
171 parameters. For motif analysis, sequence logo visualizations were performed using pLOGO with  
172 serine or threonine residues fixed at position 0. Positions with significant residue presence are  
173 depicted as amino acid letters sized above the red line (O'shea *et al.*, 2013).

#### 174 *Carotenoid analysis.*

175 Chlamydomonas cells were collected by centrifugation (4000 g for 5 min) and resuspended in 80%  
176 acetone. Samples were heat up for 5 min in a water bath at 90°C and then centrifuge at 10000g  
177 10min. The supernatant evaporated under N<sub>2</sub>, and then resuspended in 80% acetone. The  
178 separation and chromatographic analysis of pigments was performed in a HPLC using a Waters  
179 Spherisorb ODS2 column (4.6 x 250 mm, 5µm particle size). The chromatographic method  
180 described by Baroli *et al.*, 2003 (Baroli *et al.*, 2003). Pigments were eluted at a flow rate of 1.0 mL  
181 min<sup>-1</sup> with a linear gradient from 100% solvent A (acetonitrile:methanol:0.1mM Tris-HCl pH 8.0  
182 [84:2:14]) to 100% solvent B (methanol:ethyl acetate [68:32]) for 20 min, followed by 7 min of  
183 solvent B, then 1 min with a linear gradient from 100% solvent B to 100% solvent A, and finally  
184 6 min with solvent A. The carotenoids were detected at 440 nm using a Waters 2996 photodiode-  
185 array detector. The different carotenoids were identified using standards from Sigma (USA) and  
186 DHI (Germany). This analysis was normalized by dry cell weight. Dry weight was determined by  
187 filtering an exact volume of microalgae culture (30 mL) on pre-targeted glass-fiber filters (1µm  
188 pore size). The filter was washed with a solution of ammonium formate (0.5 M) to remove salts  
189 and dried at 100 °C for 24 h. The dried filters were weighed in an analytical balance and the dry  
190 weight calculated by difference.

#### 191 *SDS-PAGE and Western Blotting.*

192 Chlamydomonas cells from liquid cultures were collected by centrifugation (4000 g for 5 min),  
193 washed in 50 mM Tris-HCl (pH 7.5), 10 mM NaF, 10 mM NaN<sub>3</sub>, 10 mM p-nitrophenylphosphate,  
194 10 mM sodium pyrophosphate, and 10 mM b-glycerophosphate), and resuspended in a minimal  
195 volume of the same solution supplemented with Protease Inhibitor Cocktail (Sigma). Cells were  
196 lysed by two cycles of slow freezing to -80 °C followed by thawing at room temperature. The



197 soluble cell extract was separated from the insoluble fraction by centrifugation (15 000 g for 20  
198 min) in a microcentrifuge at 4 °C. For immunoblot analyses, total protein extracts (20 µg) were  
199 subjected to 12% SDS-PAGE and then transferred to PVDF membranes (Millipore). Anti-P-  
200 RPS6(Ser242) and anti-RPS6 primary antibodies were generated as described in Dobrenel et al.,  
201 2016 (Dobrenel *et al.*, 2016b) and produced by Proteogenix, (France). Phospho-p70 S6 kinase  
202 (Thr(P)-389) polyclonal antibody (Cell Signaling, 9205) was used as described in Xiong et al.,  
203 2012 (Xiong, Yan & Sheen, Jen, 2012). Primary antibodies were diluted 1:2000 and 1:1000  
204 respectively. Secondary anti-rabbit (Sigma) antibodies were diluted 1:5000 and 1:10 000,  
205 respectively, in phosphate-buffered saline (PBS) containing 0.1% (v/v) Tween-20 (Applichem)  
206 and 5% (w/v) milk powder. The Luminata Crescendo Millipore immunoblotting detection system  
207 (Millipore) was used to detect the proteins. Proteins were quantified with the Coomassie dye  
208 binding method (BioRad).

## 209 **Results**

### 210 *Parameter selection for TORC1-specific inhibition.*

211 Previous studies in *Chlamydomonas* have shown rapamycin drug saturation ranging from 500 nM-  
212 1µM (Crespo *et al.*, 2005). For this study, 500 nM rapamycin was selected and saturating doses  
213 for Torin1 and AZD8055 in wild-type *Chlamydomonas* strain CC-1690 were determined using  
214 serial dilutions with previously published target concentrations (Couso *et al.*, 2016). Growth  
215 inhibition saturated at 500 nM for Torin1 and 700 nM for AZD8055 (Supplemental Figure 1).

216 While reports have shown phosphorylation changes as early as 2 minutes after rapamycin  
217 treatment (Rigbolt *et al.*, 2014), a 15-minute time point was chosen based on the high number of  
218 changes seen in mammalian cell lines at this time point (Demirkan *et al.*, 2011; Harder *et al.*, 2014;  
219 Rigbolt *et al.*, 2014) and to ensure reproducibility in treatment and harvesting across 20 samples  
220 (control, AZD8055-, Torin1-, and rapamycin-treated with n=5) from the early logarithmic phase  
221 of growth. Growth for each replicate was staggered, and to limit batch-effects replicates were  
222 harvested in sets, each containing a control sample and the three different drug-tested samples  
223 (Figure 1) prior to downstream processing.

224 Prior rapamycin phosphoproteomic experiments in mammalian studies have shown that  
225 phosphopeptide ratios in general were not affected by normalization to protein levels at a 15 min

226 time point (Harder *et al.*, 2014). To confirm this in *Chlamydomonas reinhardtii*, a whole-cell  
227 proteomics experiment (n=4) was performed after 15 min of rapamycin inhibition. These results  
228 showed that protein abundance levels in general are not affected with only 18 of the 1,539 proteins  
229 quantified significantly changing (Supplemental Table S4) with no significant differences in  
230 protein abundances between control and treatment (Supplemental Figure 2). While 4 of the 18  
231 proteins changing at the protein level were identified in the phosphoproteomics study detailed  
232 below, they were not detected as phospho-modulated following chemical inhibition and thus not  
233 proteins of interest in this study. Thus, we have confidence that the statistically significant  
234 phosphorylation sites detected are from changes in the phosphorylation status and not an artefact  
235 of protein expression or turnover.

### 236 *Quantitative coverage of the TOR-inhibited phosphoproteome.*

237 Label-free quantitative phosphoproteomics was used to compare normalized abundance values of  
238 control samples (n=5) versus samples treated with each of the chemical inhibitors (n=5) using an  
239 area under the curve (AUC) MS1 intensity-based quantitation method. For this approach, the  
240 change in chromatographic peak area between control and chemically-inhibited replicates for each  
241 phosphopeptide was the basis for determining relative phosphopeptide abundance. Tip-based TiO<sub>2</sub>  
242 phosphopeptide enrichment that previously showed high reproducibility between samples (Werth  
243 *et al.*, 2017) was used for sample preparation. As part of the LFQ pipeline, quantitative data was  
244 filtered for only peptides containing a phosphorylation site on Ser, Thr, or Tyr after peak picking  
245 and peptide sequence determination. At least 3 of the 5 replicates for each condition were required  
246 to have nonzero abundances to remain in the final dataset presented in Table S1 and missing value  
247 imputation was performed on log-transformed normalized abundances (Cox & Mann, 2012;  
248 Tyanova *et al.*, 2016). Highly variable sites remaining in the dataset were then removed by filtering  
249 out those with a coefficient of variation of >25% in >2 experimental conditions. The resulting  
250 dataset contained 2,547 unique phosphosites from 1,432 different proteins (Table S1) in untreated  
251 control samples. To determine sites of interest following chemical inhibition with Torin1,  
252 AZD8055, or rapamycin, two sample Student's T-tests were performed between samples from  
253 each chemical inhibitor compared and control samples. From this, 258 phosphosites from 219  
254 phosphopeptides showed at least a two-fold change and a p-value  $\leq 0.05$  (Figure 2a, Table S2).  
255 High confidence phosphorylation site assignments (90% site-localization based on Mascot Delta

256 scoring(Savitski *et al.*, 2011)) were achieved for 48% of the dataset (1,123 of the 2,363  
257 phosphopeptides) listed in Table S1. AZD8055 treatment resulted in 97 phosphopeptides  
258 modulated in the wild-type strain (Figure 2a). A matched control experiment using an AZD-  
259 insensitive strain which grow similar to wild-type (Supplemental Figure 3) showed only 13 low  
260 abundance phosphosites differentially changing (Table S3, Figure 2b). Of the 13, no overlap was  
261 found with the 258 modulated phosphosites in the main dataset.

262 Torin1 treatment caused the largest number of significant changes with 103 up- and 57 down-  
263 modulated phosphosites. AZD8055 treatment caused 75 up- and 19 down-modulated  
264 phosphosites, while rapamycin treatment caused 40 up- and 35 down-modulated phosphosites.  
265 Overlap analysis of the differential sites for each drug revealed 88% (57/66) of all the down-  
266 modulated sites were in the Torin1 subset, while 42% (24/57) of the Torin1 down-modulated sites  
267 were not detected with AZD or rapamycin. Up-regulated sites were also compared for each  
268 condition and to determine if the conditions had significant overlap between down- and up-  
269 modulated sites, a hypergeometric test was performed with p-values of  $3.76 \times 10^{-25}$  and  $2.87 \times 10^{-34}$ ,  
270 respectively, showing significant overlap.

#### 271 *Cluster analysis and phosphosite motif identification.*

272 Kinase specificity can be dictated by amino acid residues immediately surrounding  
273 phosphorylation sites on substrates (Chou & Schwartz, 2011). Mammalian TOR has been shown  
274 to mainly (but not exclusively) phosphorylate (S/T)P motifs and motifs with hydrophobic residues  
275 surrounding the phosphorylation site making it a relatively promiscuous kinase whose substrate  
276 choices may also be influenced by additional interactions outside the phosphosite region  
277 (Robitaille *et al.*, 2013). Hierarchical clustering of *Chlamydomonas* modulated phosphosites  
278 generated 2 distinct clusters (Figure 3a,b), and motif analysis (O'shea *et al.*, 2013) was performed  
279 on decreasing (cluster 1) and increasing (cluster 2) clusters. Cluster 1 phosphosites, which  
280 contained 94% of sites that significantly decrease in phosphorylation upon TOR inhibition, had  
281 significant enrichment for a proline in the +1 position and arginine in the -3 position with respect  
282 to the phosphorylation site (position 0) that showed strong enrichment for serine over threonine  
283 (Figure 3c). Cluster 2 phosphosites also had significant enrichment for a proline in the +1 position  
284 and arginine in the -3 position in addition to enrichment for an aspartic acid at the +3 position.  
285 Thus, CrTOR may have a preference for phosphorylation of (S/T)P motifs on substrates, similar

286 to mTOR(Robitaille *et al.*, 2013) and other diverse proline-directed kinases including cyclin-  
287 dependent protein kinases (CDKs) and mitogen-activated protein kinases (MAPKs) (Lu *et al.*,  
288 2002). Additionally, a phosphoproteomic study using mammalian cell line MCF7 identified the  
289 RXXS/TP motif identified in clusters 1 and 2 as a rapamycin-sensitive motif (Rigbolt *et al.*, 2014).  
290 Other studies have also found RXRXXS/T and RXXS/T motifs (Demirkan *et al.*, 2011; Harder *et*  
291 *al.*, 2014) enriched among rapamycin-sensitive phosphosites that are recognized by mTOR-  
292 regulated kinases Akt, S6K1 and SGK1 (Hsu *et al.*, 2011). Cluster 2 additionally has an acidic  
293 motif also found in casein kinase- II substrates (Lv *et al.*, 2014).

#### 294 *Phosphosites in TORC1 complex proteins.*

295 Numerous phosphosites in mammalian homologs of TORC1 complex proteins are regulated by  
296 the TOR pathway and/or are phosphorylated autocatalytically (Foster *et al.*, 2010). This includes  
297 sites on Raptor and mTOR homologs. Therefore, phosphosites found on CrTORC1 complex  
298 proteins could be affected by TOR inhibition. TORC1 complex proteins conserved in  
299 *Chlamydomonas* include TOR (Cre09.g400553.t1.1), Raptor (Cre08.g371957.t1.1), and LST8  
300 (Cre17.g713900.t1.2) (Merchant *et al.*, 2007; Diaz-Troya *et al.*, 2008; Perez-Perez *et al.*, 2010;  
301 Couso *et al.*, 2016). While there is a known LST8 homolog in *Chlamydomonas*, it is not known to  
302 be phosphorylated (Wang *et al.*, 2014). Phosphosites on Raptor (Ser782/783:NL) (Not  
303 Localized:NL) and TOR (Ser2598) were detected in this study, however no statistically significant  
304 modulation in their abundance was detected. BLASTP alignment of human Raptor (Uniprot  
305 Q8N122) with CrRaptor revealed high sequence overlap on the N-terminal region of the protein  
306 (residues 9-627 with 57% identity), however known TORC1-sensitive phosphosites in the human  
307 Raptor homolog (i.e. Ser719, Ser721, Ser722, Ser859, and Ser863 (Carrière *et al.*, 2008; Foster *et*  
308 *al.*, 2010)) were not conserved in CrRaptor. Similarly, human mTOR (Uniprot P42345)  
309 phosphosites Ser2159/Thr2164 that are within the kinase domain promoting mTORC1-associated  
310 mTOR Ser2481 autophosphorylation (Ekim *et al.*, 2011) are not conserved in CrTOR. The limited  
311 sequence conservation among CrTORC1 phosphosites with mammalian TOR phosphosites  
312 precludes any predictions about functions of CrTORC1 protein phosphorylation. Other  
313 phosphosites on CrTORC1 complex proteins that were detected in previous work on the global  
314 phosphoproteome in *Chlamydomonas* (Wang *et al.*, 2014) might be significant for regulation but  
315 they were not observed in our data. Future experiments with additional fractionation to increase

316 the dynamic range of quantitative coverage could allow for deeper coverage and more  
317 comprehensive detection of phosphosites.

## 318 **Discussion**

319 *Sites modulated by TORC1 inhibition – known and putative substrates.*

320 In animal cells TORC1-inhibition blocks phosphorylation of multiple substrates including S6  
321 kinases and eukaryotic translation initiation factors, leading to a reduction in translation initiation  
322 rates for a subset of mRNAs (Jefferies *et al.*, 1994; Terada *et al.*, 1994; Wang & Proud, 2009).  
323 Phosphorylation of Ser371 and Thr389 in human p70S6K1 (Uniprot P23443-2) are reduced by  
324 treatment of cells with TOR inhibitors (Dennis *et al.*, 1996; Burnett *et al.*, 1998). While we  
325 identified one potential site (site was not localized) (Thr771/Ser773/Thr777:NL) on a  
326 Chlamydomonas homolog of ribosomal protein S6 kinase (S6K; Cre13.g579200.t1.2), its  
327 phosphorylation state was not significantly altered by TOR inhibitors (Table 1). No coverage was  
328 obtained on predicted conserved sites Ser915 and Thr932, which align to human p70S6K1 Ser371  
329 and Thr389, respectively, although these sites have been detected previously in Chlamydomonas  
330 (Wang *et al.*, 2014). Moreover, while commercial anti-phospho S6K antibodies have been shown  
331 to detect phospho-S6K in plants (Xiong, Yan & Sheen, Jen, 2012; Ahn *et al.*, 2014) they have not  
332 detected a signal in Chlamydomonas in our hands (Supplemental Figure 4) and in another study  
333 (Couso *et al.*, 2016), thus limiting our ability to independently validate Chlamydomonas TOR  
334 substrate phosphopeptides. On the other hand, Chlamydomonas ribosomal protein S6 (RPS6,  
335 Cre09.g400650.t1.2), a predicted target of S6K, showed a 2.1-fold decrease in phosphorylation on  
336 Thr127 following Torin1 treatment (Figure 5, Table 1). While this site is potentially TORC1-  
337 regulated, antibodies specific for this phosphosite needed for validation are not available. In  
338 Arabidopsis, a phosphosite on the C-terminal extremity peptide of RPS6, Ser240, had decreased  
339 phosphorylation following TOR inactivation (Dobrenel *et al.*, 2016b). While this exact site is not  
340 conserved in Chlamydomonas, the phosphoserine next to it, Ser241 in Arabidopsis (aligning to  
341 Ser242 in Chlamydomonas) has been detected in prior work (Wang *et al.*, 2014); however it was  
342 not detected in this study (Figure 4a). To determine if Ser242 in Chlamydomonas is TORC1-  
343 regulated, a western blot of proteins fractionated from wild-type cells under different drug  
344 treatments for 0, 5, 15, 30, and 60 min was performed with antibodies raised for phosphorylated  
345 and non-phosphorylated Ser242 (Figure 4b), the latter used as a control for monitoring protein

346 level. Interestingly, this site does not seem to change drastically with Torin1, AZD8055, or  
347 rapamycin treatment contrary to results on the C-terminal phosphosite in Arabidopsis.

348 *Sites modulated by TORC1 inhibition – known TOR pathway association.*

349 Of the 258 phosphosites detected as significantly modulated in this study, 10 are in homologs of  
350 proteins associated with the TOR signaling pathway (Figure 5, Table 1). In addition to four sites  
351 of decreasing phosphorylation, six proteins related to the TOR pathway had an increase in protein  
352 phosphorylation following chemical inhibition. While initially an unexpected observation, similar  
353 increases were previously reported for some phosphosites in a phosphoproteomic study of TOR  
354 inhibition in mouse liver (Demirkan *et al.*, 2011). In our study, sites with increasing  
355 phosphorylation after TOR inhibition include elongation factor 2 (EEF2, Cre12.g516200.t1.2)  
356 whose animal homologs showed reduced activity upon phosphorylation. In human cells,  
357 phosphorylation of EEF2 Thr57 by elongation factor 2 kinase (EEF2K, Cre17.g721850.t1.2)  
358 inactivates EEF2 activity, an essential factor for protein synthesis (Hizli *et al.*, 2013). This site is  
359 conserved in Chlamydomonas EEF2 (Thr57/Thr59:NL) where we detect a 4.75-fold increase in  
360 phosphorylation with AZD8055 treatment with a predicted effect of reduced translation initiation  
361 rates. From these data we predict that CrTOR signaling may inhibit EEF2 kinase activity, and that  
362 this inhibition is relieved in the presence of TOR inhibitors.

363 LA RNA-binding protein (LARP1, Cre10.g441200.t1.2) had two phosphosites that both  
364 underwent large decreases in phosphorylation upon treatment with the three chemical inhibitors.  
365 Ser817 was decreased 0.06<sub>AZD8055</sub>, 0.05<sub>Torin1</sub>, and 0.13<sub>RAP</sub> and Ser 737/738:NL was decreased  
366 0.08<sub>AZD8055</sub> and 0.01<sub>Torin 1</sub> but no change in rapamycin (0.99<sub>RAP</sub>) (Figure 5). In mammals, LARP1  
367 phosphorylation also requires mTORC1 (Hsu *et al.*, 2011; Yu *et al.*, 2011; Kang *et al.*, 2013) with  
368 studies in human cell lines establishing LARP1 as a target of mTORC1 and S6K with non-  
369 phosphorylated LARP1 interacting with both 5' and 3' UTRs of RP mRNAs and inhibiting their  
370 translation (Hong *et al.*, 2017). Additional reports have shown LARP1 as a direct substrate of  
371 mTORC1 in mammalian cells with mTORC1 controlling Terminal Oligopyrimidine (TOP)  
372 mRNA translation via LARP1 (Fonseca *et al.*, 2015; Hong *et al.*, 2017). The dramatic modulation  
373 of LARP1 phosphorylation detected in our study indicates that LARP1 may have a parallel role in  
374 Chlamydomonas. The human LARP1 phosphosites are not conserved with those we found in  
375 Chlamydomonas. However, based on the NCBI conserved domain searching (Marchler-Bauer &

376 Bryant, 2004), the DM15 domain required for the interaction of LARP1 with mTORC1 in human  
377 cell lines is conserved in *Chlamydomonas* LARP1, and the phospho-Ser817 detected in our study  
378 is adjacent to the DM15 domain (877-915) in *Chlamydomonas*, a region in mammalian  
379 LARP1 shown to be required for interaction with mTORC1 (Hong *et al.*, 2017).

#### 380 *Additional proteins with phosphosites altered by TORC1 inhibition*

381 The majority of differential phosphosites we identified were not previously linked to TOR  
382 signaling, including in *Chlamydomonas*. These include sites on a translation-related protein  
383 (Cre17.g696250.t1.1) and RNA-binding proteins (Cre10.g441200.t1.2, Cre10.g466450.t1.1,  
384 Cre16.g659150.t1.1, Cre16.g662702.t1.1 Cre17.g729150.t1.2). One of the most down-modulated  
385 proteins annotated as CTC-interacting domain 4 (CID4, Cre01.g063997.t1.1), has been shown to  
386 have an important function in regulation of translation and mRNA stability in eukaryotes (Bravo  
387 *et al.*, 2005; Jiménez-López *et al.*, 2015). CID4 had 2 sites, Ser441 (FC=0.2<sub>AZD8055</sub>, FC=0.14<sub>TORIN1</sub>)  
388 and Ser439/Ser441/Ser446:NL (FC=0.03<sub>AZD8055</sub>, FC=0.05<sub>TORIN1</sub>) with a large decrease in  
389 phosphorylation upon inhibitor treatment. While little is known about the relationship between this  
390 protein and TORC1 signaling, the CTC domain, more recently referred to as the MLLC domain  
391 (Jiménez-López & Guzmán, 2014), is also found in evolutionarily conserved Poly (A)-binding  
392 proteins (PABPs). The large decrease in CID4 phosphorylation seen upon inhibition of the  
393 CrTORC1 pathway in our study implies a potential role for TORC1 mediated control of  
394 translation, similar to other well-known TOR substrates.

395 Another differential phosphosite of interest following TORC1 inhibition that was not previously  
396 linked to TOR regulation is a site on lycopene beta/epsilon cyclase protein (Cre04.g221550.t1.2--  
397 Thr800/Ser802:NL). This phosphosite is significantly increased upon Torin1 treatment (FC=4.02)  
398 and the total protein level remained constant upon rapamycin treatment (Supplementary Table S4,  
399 FC=0.88). Lycopene beta/epsilon cyclases are required for carotenoid biosynthesis, carrying out  
400 cyclation of lycopene to yield  $\alpha$ - and  $\beta$ - carotenes (Cunningham *et al.*, 1996; Cunningham & Gantt,  
401 2001; Cordero *et al.*, 2010) which have been shown to be high-value compounds participating in  
402 light harvesting and in the protection of the photosynthetic apparatus against photo-oxidation  
403 damage (Frank & Cogdell, 1996; Cunningham Jr & Gantt, 1998). Recently in rice, carotenoid  
404 content was shown to be significantly lower in an *s6k1* mutant compared to wild-type (Sun *et al.*,  
405 2016) revealing a potential connection between the TOR pathway and carotenoid production. To

406 further investigate the effect of TORC1 inhibition on carotenoid biosynthesis in *Chlamydomonas*  
407 based on our phosphoproteomic finding, carotenoid levels in AZD-, Torin1- and rapamycin-treated  
408 cells were assessed after eight hours of treatment with three biological and two technical replicates  
409 (Figure 6, Table 2). After eight hours of treatment, there was a significant increase in various  
410 carotenoids measured in TOR-inhibited samples including  $\beta$ -carotene, which is directly  
411 downstream of cyclase activity (Figure 6, Table 2). While the effects on carotenoid biosynthesis  
412 and secondary metabolism following TORC1 inhibition required eight hours to become detectable,  
413 this is the first evidence that carotenoid production is modulated by TOR signaling in algae.  
414 Additionally, altered cyclase protein levels are not likely responsible for this finding since previous  
415 studies showed no change in lycopene beta/epsilon cyclase protein level after up to 24 hours of  
416 nitrogen stress (Cunningham Jr & Gantt, 1998; Valledor *et al.*, 2014), a condition that is  
417 metabolically similar to TOR inhibition (Perez-Perez *et al.*, 2010; Roustan *et al.*, 2017).

418 Numerous phosphosites from proteins without Phytozome database descriptions were also found  
419 to be down-regulated upon CrTORC1 inhibition, including some sites with large decreases (>five-  
420 fold). For all unannotated proteins, we searched for pfam, Panther, KOG, KEGG, KO, and GO  
421 pathway terms and domain conservation using Phytozome and NCBI annotations (Table S4).  
422 Numerous proteins had conserved domains including structural maintenance of chromosomes  
423 (Accession: cl25732), autophagy protein (Accession: cl27196), transmembrane proteins  
424 (Accession: cl24526), and small acidic protein (Accession: pfam15477). While the large changes  
425 upon chemical inhibition are potentially interesting, especially the five proteins containing sites  
426 with at least a five-fold decrease in phosphorylation (Cre03.g152150.t1.2, Cre06.g263250.t1.1,  
427 Cre11.g469150.t1.2, Cre05.g236650.t1.1, Cre13.g582800.t1.2), future targeted work would be  
428 required to infer biological significance to this observation. To aid in this, the fifty-eight modulated  
429 sites without Phytozome database annotation were also homology searched for best BLAST hit  
430 IDs in *Volvox*, *Gonium*, and *Arabidopsis* to find homologs among green lineage (Table S5) and  
431 Table S2 displays all of the experimentally derived sites modulated by AZD8055, Torin1, and/or  
432 rapamycin and will serve as a guide in follow-up studies.

433 In summary, we obtained a candidate list of phosphosites modulated following TORC1  
434 inhibition. We achieved extensive coverage of the TOR-modulated phosphoproteome in  
435 *Chlamydomonas* using a quantitative label-free approach. Our approach was validated by the



436 overlap of phosphosites altered using different TOR inhibitors and by our identification of  
437 Chlamydomonas homologs of TOR signaling-related proteins such as RPS6 and LARP1 that had  
438 decreased phosphorylation upon TORC1 inhibition. Follow-up experiments guided by our  
439 phosphoproteomic findings in lycopene beta/epsilon cyclase showed that carotenoid levels are  
440 affected by TORC1 inhibition, the first evidence that carotenoid production is under TOR control  
441 in algae. Conserved TOR substrate motifs were also identified such as RXXS/TP and RXXS/TP.  
442 Our study provides a new resource for investigating the phosphorylation networks governed by  
443 the TOR kinase pathway in Chlamydomonas.

#### 444 Acknowledgements

445 This research was supported by a National Science Foundation CAREER award (MCB-  
446 1552522) awarded to L.M.H.

#### 447 Author contributions:

448 E.G.W., L.M.H., I.C.L., J.G.U., J.L.C. contributed to planning and experimental design. E.G.W.,  
449 I.C.L., and Z.P. performed experiments. E.G.W., E.W.M. performed data analysis. E.G.W.,  
450 L.M.H., J.G.U wrote the manuscript.

451

452 References

- 453
- 454 **Ahn CS, Ahn H-K, Pai H-S. 2014.** Overexpression of the PP2A regulatory subunit Tap46 leads to  
455 enhanced plant growth through stimulation of the TOR signalling pathway. *Journal of*  
456 *experimental botany* **66**(3): 827-840.
- 457 **Ashburner M, Ball CA, Blake JA, Botstein D, Butler H, Cherry JM, Davis AP, Dolinski K, Dwight**  
458 **SS, Eppig JT. 2000.** Gene Ontology: tool for the unification of biology. *Nature genetics* **25**(1):  
459 25-29.
- 460 **Baroli I, Do AD, Yamane T, Niyogi KK. 2003.** Zeaxanthin accumulation in the absence of a functional  
461 xanthophyll cycle protects *Chlamydomonas reinhardtii* from photooxidative stress. *The Plant Cell*  
462 **15**(4): 992-1008.
- 463 **Benjamin D, Colombi M, Moroni C, Hall MN. 2011.** Rapamycin passes the torch: a new generation of  
464 mTOR inhibitors. *Nature reviews Drug discovery* **10**(11): 868.
- 465 **Bravo J, Aguilar-Henonin L, Olmedo G, Guzman P. 2005.** Four distinct classes of proteins as  
466 interaction partners of the PABC domain of *Arabidopsis thaliana* Poly (A)-binding proteins.  
467 *Molecular genetics and genomics* **272**(6): 651-665.
- 468 **Brown EJ, Albers MW, Shin TB, Keith CT, Lane WS, Schreiber SL. 1994.** A mammalian protein  
469 targeted by G1-arresting rapamycin-receptor complex. *Nature* **369**(6483): 756-758.
- 470 **Burnett PE, Barrow RK, Cohen NA, Snyder SH, Sabatini DM. 1998.** RAFT1 phosphorylation of the  
471 translational regulators p70 S6 kinase and 4E-BP1. *Proceedings of the national academy of*  
472 *sciences* **95**(4): 1432-1437.
- 473 **Carrière A, Cargnello M, Julien L-A, Gao H, Bonneil É, Thibault P, Roux PP. 2008.** Oncogenic  
474 MAPK signaling stimulates mTORC1 activity by promoting RSK-mediated raptor  
475 phosphorylation. *Current biology* **18**(17): 1269-1277.
- 476 **Chou MF, Schwartz D. 2011.** Biological sequence motif discovery using motif-x. *Current Protocols in*  
477 *Bioinformatics*: 13.15. 11-13.15. 24.
- 478 **Chresta CM, Davies BR, Hickson I, Harding T, Cosulich S, Critchlow SE, Vincent JP, Ellston R,**  
479 **Jones D, Sini P, et al. 2010.** AZD8055 is a potent, selective, and orally bioavailable ATP-  
480 competitive mammalian target of rapamycin kinase inhibitor with in vitro and in vivo antitumor  
481 activity. *Cancer Res* **70**(1): 288-298.
- 482 **Cordero BF, Obraztsova I, Martín L, Couso I, León R, Ángeles Vargas M, Rodríguez H. 2010.**  
483 ISOLATION AND CHARACTERIZATION OF A LYCOPENE  $\beta$ -CYCLASE GENE FROM  
484 THE ASTAXANTHIN-PRODUCING GREEN ALGA *CHLORELLA ZOFINGIENSIS*  
485 (CHLOROPHYTA). *Journal of phycology* **46**(6): 1229-1238.
- 486 **Couso I, Evans BS, Li J, Liu Y, Ma F, Diamond S, Allen DK, Umen JG. 2016.** Synergism between  
487 Inositol Polyphosphates and TOR Kinase Signaling in Nutrient Sensing, Growth Control, and  
488 Lipid Metabolism in *Chlamydomonas*. *The Plant Cell* **28**(9): 2026-2042.
- 489 **Cox J, Mann M. 2012.** 1D and 2D annotation enrichment: a statistical method integrating quantitative  
490 proteomics with complementary high-throughput data. *BMC bioinformatics* **13**(16): S12.
- 491 **Crespo JL, Diaz-Troya S, Florencio FJ. 2005.** Inhibition of target of rapamycin signaling by rapamycin  
492 in the unicellular green alga *Chlamydomonas reinhardtii*. *Plant Physiol* **139**(4): 1736-1749.
- 493 **Cunningham FX, Gantt E. 2001.** One ring or two? Determination of ring number in carotenoids by  
494 lycopene  $\epsilon$ -cyclases. *Proceedings of the national academy of sciences* **98**(5): 2905-2910.
- 495 **Cunningham FX, Pogson B, Sun Z, McDonald KA, DellaPenna D, Gantt E. 1996.** Functional analysis  
496 of the beta and epsilon lycopene cyclase enzymes of *Arabidopsis* reveals a mechanism for control  
497 of cyclic carotenoid formation. *The Plant Cell* **8**(9): 1613-1626.
- 498 **Cunningham Jr F, Gantt E. 1998.** Genes and enzymes of carotenoid biosynthesis in plants. *Annual*  
499 *review of plant biology* **49**(1): 557-583.
- 500 **Demirkan G, Yu K, Boylan JM, Salomon AR, Gruppuso PA. 2011.** Phosphoproteomic profiling of in  
501 vivo signaling in liver by the mammalian target of rapamycin complex 1 (mTORC1). *PLoS One*  
502 **6**(6): e21729.

- 503 **Dennis PB, Pullen N, Kozma SC, Thomas G. 1996.** The principal rapamycin-sensitive p70 (s6k)  
504 phosphorylation sites, T-229 and T-389, are differentially regulated by rapamycin-insensitive  
505 kinase kinases. *Molecular and cellular biology* **16**(11): 6242-6251.
- 506 **Diaz-Troya S, Florencio FJ, Crespo JL. 2008.** Target of rapamycin and LST8 proteins associate with  
507 membranes from the endoplasmic reticulum in the unicellular green alga *Chlamydomonas*  
508 *reinhardtii*. *Eukaryot Cell* **7**(2): 212-222.
- 509 **Dibble CC, Manning BD. 2013.** Signal integration by mTORC1 coordinates nutrient input with  
510 biosynthetic output. *Nat Cell Biol* **15**(6): 555-564.
- 511 **Dobrenel T, Caldana C, Hanson J, Robaglia C, Vincentz M, Veit B, Meyer C. 2016a.** TOR Signaling  
512 and Nutrient Sensing. *Annual review of plant biology* **67**: 261-285.
- 513 **Dobrenel T, Mancera-Martínez E, Forzani C, Azzopardi M, Davanture M, Moreau M,**  
514 **Schepetilnikov M, Chicher J, Langella O, Zivy M. 2016b.** The Arabidopsis TOR kinase  
515 specifically regulates the expression of nuclear genes coding for plastidic ribosomal proteins and  
516 the phosphorylation of the cytosolic ribosomal protein S6. *Frontiers in plant science* **7**: 1611.
- 517 **Dobrenel T, Marchive C, Sormani R, Moreau M, Mozzo M, Montane MH, Menand B, Robaglia C,**  
518 **Meyer C. 2011.** Regulation of plant growth and metabolism by the TOR kinase. *Biochem Soc*  
519 *Trans* **39**(2): 477-481.
- 520 **Ekim B, Magnuson B, Acosta-Jaquez HA, Keller JA, Feener EP, Fingar DC. 2011.** mTOR kinase  
521 domain phosphorylation promotes mTORC1 signaling, cell growth, and cell cycle progression.  
522 *Molecular and cellular biology* **31**(14): 2787-2801.
- 523 **Fingar DC, Blenis J. 2004.** Target of rapamycin (TOR): an integrator of nutrient and growth factor  
524 signals and coordinator of cell growth and cell cycle progression. *Oncogene* **23**(18): 3151-3171.
- 525 **Fonseca BD, Zakaria C, Jia J-J, Graber TE, Svitkin Y, Tahmasebi S, Healy D, Hoang H-D, Jensen**  
526 **JM, Diao IT. 2015.** La-related protein 1 (LARP1) represses terminal oligopyrimidine (TOP)  
527 mRNA translation downstream of mTOR complex 1 (mTORC1). *Journal of Biological*  
528 *Chemistry* **290**(26): 15996-16020.
- 529 **Foster KG, Acosta-Jaquez HA, Romeo Y, Ekim B, Soliman GA, Carriere A, Roux PP, Ballif BA,**  
530 **Fingar DC. 2010.** Regulation of mTOR complex 1 (mTORC1) by raptor Ser863 and multisite  
531 phosphorylation. *J Biol Chem* **285**(1): 80-94.
- 532 **Frank HA, Cogdell RJ. 1996.** Carotenoids in photosynthesis. *Photochemistry and photobiology* **63**(3):  
533 257-264.
- 534 **González A, Hall MN. 2017.** Nutrient sensing and TOR signaling in yeast and mammals. *The EMBO*  
535 *journal*: e201696010.
- 536 **Harder LM, Bunkenborg J, Andersen JS. 2014.** Inducing autophagy: a comparative phosphoproteomic  
537 study of the cellular response to ammonia and rapamycin. *Autophagy* **10**(2): 339-355.
- 538 **Heitman J, Movva NR, Hall MN. 1991.** Targets for cell cycle arrest by the immunosuppressant  
539 rapamycin in yeast. *Science* **253**(5022): 905-909.
- 540 **Hizli AA, Chi Y, Swanger J, Carter JH, Liao Y, Welcker M, Ryazanov AG, Clurman BE. 2013.**  
541 Phosphorylation of eukaryotic elongation factor 2 (eEF2) by cyclin A–cyclin-dependent kinase 2  
542 regulates its inhibition by eEF2 kinase. *Molecular and cellular biology* **33**(3): 596-604.
- 543 **Hong S, Freeberg MA, Han T, Kamath A, Yao Y, Fukuda T, Suzuki T, Kim JK, Inoki K. 2017.**  
544 LARP1 functions as a molecular switch for mTORC1-mediated translation of an essential class of  
545 mRNAs. *eLife* **6**.
- 546 **Hsu PP, Kang SA, Rameseder J, Zhang Y, Ottina KA, Lim D, Peterson TR, Choi Y, Gray NS,**  
547 **Yaffe MB, et al. 2011.** The mTOR-regulated phosphoproteome reveals a mechanism of  
548 mTORC1-mediated inhibition of growth factor signaling. *Science* **332**(6035): 1317-1322.
- 549 **Imamura S, Kawase Y, Kobayashi I, Shimojima M, Ohta H, Tanaka K. 2016.** TOR (target of  
550 rapamycin) is a key regulator of triacylglycerol accumulation in microalgae. *Plant signaling &*  
551 *behavior* **11**(3): e1149285.

- 552 **Imamura S, Kawase Y, Kobayashi I, Sone T, Era A, Miyagishima S-y, Shimojima M, Ohta H,**  
553 **Tanaka K. 2015.** Target of rapamycin (TOR) plays a critical role in triacylglycerol accumulation  
554 in microalgae. *Plant molecular biology* **89**(3): 309-318.
- 555 **Jefferies H, Reinhard C, Kozma S, Thomas G. 1994.** Rapamycin selectively represses translation of  
556 the " polypyrimidine tract" mRNA family. *Proceedings of the national academy of sciences*  
557 **91**(10): 4441-4445.
- 558 **Jiménez-López D, Bravo J, Guzmán P. 2015.** Evolutionary history exposes radical diversification  
559 among classes of interaction partners of the MLE domain of plant poly (A)-binding proteins.  
560 *BMC evolutionary biology* **15**(1): 195.
- 561 **Jiménez-López D, Guzmán P. 2014.** Insights into the evolution and domain structure of Ataxin-2  
562 proteins across eukaryotes. *BMC research notes* **7**(1): 453.
- 563 **Käll L, Canterbury JD, Weston J, Noble WS, MacCoss MJ. 2007.** Semi-supervised learning for  
564 peptide identification from shotgun proteomics datasets. *Nature Methods* **4**(11): 923-925.
- 565 **Kanehisa M, Goto S. 2000.** KEGG: kyoto encyclopedia of genes and genomes. *Nucleic acids research*  
566 **28**(1): 27-30.
- 567 **Kang SA, Pacold ME, Cervantes CL, Lim D, Lou HJ, Ottina K, Gray NS, Turk BE, Yaffe MB,**  
568 **Sabatini DM. 2013.** mTORC1 phosphorylation sites encode their sensitivity to starvation and  
569 rapamycin. *Science* **341**(6144): 1236566.
- 570 **Liu Q, Xu C, Kirubakaran S, Zhang X, Hur W, Liu Y, Kwiatkowski NP, Wang J, Westover KD,**  
571 **Gao P. 2013.** Characterization of Torin2, an ATP-competitive inhibitor of mTOR, ATM, and  
572 ATR. *Cancer research* **73**(8): 2574-2586.
- 573 **Loewith R, Hall MN. 2011.** Target of rapamycin (TOR) in nutrient signaling and growth control.  
574 *Genetics* **189**(4): 1177-1201.
- 575 **Lu KP, Liou Y-C, Zhou XZ. 2002.** Pinning down proline-directed phosphorylation signaling. *Trends in*  
576 *cell biology* **12**(4): 164-172.
- 577 **Lv D-W, Ge P, Zhang M, Cheng Z-W, Li X-H, Yan Y-M. 2014.** Integrative network analysis of the  
578 signaling cascades in seedling leaves of bread wheat by large-scale phosphoproteomic profiling.  
579 *Journal of proteome research* **13**(5): 2381-2395.
- 580 **Marchler-Bauer A, Bryant SH. 2004.** CD-Search: protein domain annotations on the fly. *Nucleic acids*  
581 *research* **32**(suppl\_2): W327-W331.
- 582 **Menand B, Desnos T, Nussaume L, Berger F, Bouchez D, Meyer C, Robaglia C. 2002.** Expression  
583 and disruption of the Arabidopsis TOR (target of rapamycin) gene. *Proc Natl Acad Sci U S A*  
584 **99**(9): 6422-6427.
- 585 **Merchant SS, Prochnik SE, Vallon O, Harris EH, Karpowicz SJ, Witman GB, Terry A, Salamov A,**  
586 **Fritz-Laylin LK, Maréchal-Drouard L. 2007.** The Chlamydomonas genome reveals the  
587 evolution of key animal and plant functions. *Science* **318**(5848): 245-250.
- 588 **Montane MH, Menand B. 2013.** ATP-competitive mTOR kinase inhibitors delay plant growth by  
589 triggering early differentiation of meristematic cells but no developmental patterning change. *J*  
590 *Exp Bot* **64**(14): 4361-4374.
- 591 **O'shea JP, Chou MF, Quader SA, Ryan JK, Church GM, Schwartz D. 2013.** pLogo: a probabilistic  
592 approach to visualizing sequence motifs. *Nature Methods* **10**(12): 1211.
- 593 **Pérez-Pérez ME, Couso I, Crespo JL. 2017.** The TOR Signaling Network in the Model Unicellular  
594 Green Alga Chlamydomonas reinhardtii. *Biomolecules* **7**(3): 54.
- 595 **Perez-Perez ME, Florencio FJ, Crespo JL. 2010.** Inhibition of target of rapamycin signaling and stress  
596 activate autophagy in Chlamydomonas reinhardtii. *Plant Physiol* **152**(4): 1874-1888.
- 597 **Raught B, Gingras AC, Sonenberg N. 2001.** The target of rapamycin (TOR) proteins. *Proc Natl Acad*  
598 *Sci U S A* **98**(13): 7037-7044.
- 599 **Ren M, Venglat P, Qiu S, Feng L, Cao Y, Wang E, Xiang D, Wang J, Alexander D, Chalivendra S,**  
600 **et al. 2012.** Target of rapamycin signaling regulates metabolism, growth, and life span in  
601 Arabidopsis. *Plant Cell* **24**(12): 4850-4874.

- 602 **Rigbolt KT, Zarei M, Sprenger A, Becker AC, Diedrich B, Huang X, Eiselein S, Kristensen AR,**  
603 **Gretzmeier C, Andersen JS, et al. 2014.** Characterization of early autophagy signaling by  
604 quantitative phosphoproteomics. *Autophagy* **10**(2): 356-371.
- 605 **Robitaille AM, Christen S, Shimobayashi M, Cornu M, Fava LL, Moes S, Prescianotto-Baschong**  
606 **C, Sauer U, Jenoe P, Hall MN. 2013.** Quantitative phosphoproteomics reveal mTORC1  
607 activates de novo pyrimidine synthesis. *Science* **339**(6125): 1320-1323.
- 608 **Rodrigues SP, Alvarez S, Werth EG, Slade WO, Gau B, Cahoon EB, Hicks LM. 2015.** Multiplexing  
609 strategy for simultaneous detection of redox-, phospho- and total proteome – understanding TOR  
610 regulating pathways in *Chlamydomonas reinhardtii*. *Anal. Methods* **7**(17): 7336-7344.
- 611 **Roohi A, Hojjat-Farsangi M. 2017.** Recent advances in targeting mTOR signaling pathway using small  
612 molecule inhibitors. *Journal of drug targeting* **25**(3): 189-201.
- 613 **Roustan V, Bakhtiari S, Roustan P-J, Weckwerth W. 2017.** Quantitative in vivo phosphoproteomics  
614 reveals reversible signaling processes during nitrogen starvation and recovery in the biofuel  
615 model organism *Chlamydomonas reinhardtii*. *Biotechnology for biofuels* **10**(1): 280.
- 616 **Sabatini DM, Erdjument-Bromage H, Lui M, Tempst P, Snyder SH. 1994.** RAFT1: a mammalian  
617 protein that binds to FKBP12 in a rapamycin-dependent fashion and is homologous to yeast  
618 TORs. *Cell* **78**(1): 35-43.
- 619 **Savitski MM, Lemeer S, Boesche M, Lang M, Mathieson T, Bantscheff M, Kuster B. 2011.**  
620 Confident phosphorylation site localization using the Mascot Delta Score. *Molecular & Cellular*  
621 *Proteomics* **10**(2): M110. 003830.
- 622 **Saxton RA, Sabatini DM. 2017.** mTOR signaling in growth, metabolism, and disease. *Cell* **168**(6): 960-  
623 976.
- 624 **Slade WO, Werth EG, McConnell EW, Alvarez S, Hicks LM. 2015.** Quantifying reversible oxidation  
625 of protein thiols in photosynthetic organisms. *J Am Soc Mass Spectrom* **26**(4): 631-640.
- 626 **Sun L, Yu Y, Hu W, Min Q, Kang H, Li Y, Hong Y, Wang X, Hong Y. 2016.** Ribosomal protein S6  
627 kinase1 coordinates with TOR-Raptor2 to regulate thylakoid membrane biosynthesis in rice.  
628 *Biochimica et Biophysica Acta (BBA)-Molecular and Cell Biology of Lipids* **1861**(7): 639-649.
- 629 **Terada N, Patel HR, Takase K, Kohno K, Nairn AC, Gelfand EW. 1994.** Rapamycin selectively  
630 inhibits translation of mRNAs encoding elongation factors and ribosomal proteins. *Proceedings*  
631 *of the national academy of sciences* **91**(24): 11477-11481.
- 632 **Thoreen CC, Kang SA, Chang JW, Liu Q, Zhang J, Gao Y, Reichling LJ, Sim T, Sabatini DM,**  
633 **Gray NS. 2009.** An ATP-competitive mammalian target of rapamycin inhibitor reveals  
634 rapamycin-resistant functions of mTORC1. *J Biol Chem* **284**(12): 8023-8032.
- 635 **Tyanova S, Temu T, Sinitcyn P, Carlson A, Hein MY, Geiger T, Mann M, Cox J. 2016.** The Perseus  
636 computational platform for comprehensive analysis of (prote) omics data. *Nature Methods* **13**(9):  
637 731-740.
- 638 **Valledor L, Furuhashi T, Recuenco-Muñoz L, Wienkoop S, Weckwerth W. 2014.** System-level  
639 network analysis of nitrogen starvation and recovery in *Chlamydomonas reinhardtii* reveals  
640 potential new targets for increased lipid accumulation. *Biotechnology for biofuels* **7**(1): 171.
- 641 **van Dam TJ, Zwartkruis FJ, Bos JL, Snel B. 2011.** Evolution of the TOR pathway. *J Mol Evol* **73**(3-  
642 4): 209-220.
- 643 **Vizcaíno JA, Côté RG, Csordas A, Dienes JA, Fabregat A, Foster JM, Griss J, Alpi E, Birim M,**  
644 **Contell J. 2013.** The PRoteomics IDentifications (PRIDE) database and associated tools: status  
645 in 2013. *Nucleic acids research* **41**(D1): D1063-D1069.
- 646 **Wang H, Gau B, Slade WO, Juergens M, Li P, Hicks LM. 2014.** The global phosphoproteome of  
647 *Chlamydomonas reinhardtii* reveals complex organellar phosphorylation in the flagella and  
648 thylakoid membrane. *Molecular & Cellular Proteomics* **13**(9): 2337-2353.
- 649 **Wang X, Proud CG. 2009.** Nutrient control of TORC1, a cell-cycle regulator. *Trends in cell biology*  
650 **19**(6): 260-267.
- 651 **Werth EG, McConnell EW, Gilbert TSK, Couso Lianez I, Perez CA, Manley CK, Graves LM,**  
652 **Umen JG, Hicks LM. 2017.** Probing the global kinome and phosphoproteome in

653 Chlamydomonas reinhardtii via sequential enrichment and quantitative proteomics. *The Plant*  
654 *Journal* **89**(2): 416-426.

655 **Wullschleger S, Loewith R, Hall MN. 2006.** TOR signaling in growth and metabolism. *Cell* **124**(3):  
656 471-484.

657 **Xiong Y, McCormack M, Li L, Hall Q, Xiang C, Sheen J. 2013.** Glucose-TOR signalling reprograms  
658 the transcriptome and activates meristems. *Nature* **496**(7444): 181-186.

659 **Xiong Y, Sheen J. 2012.** Rapamycin and glucose-target of rapamycin (TOR) protein signaling in plants.  
660 *Journal of Biological Chemistry* **287**(4): 2836-2842.

661 **Xiong Y, Sheen J. 2012.** Rapamycin and glucose-target of rapamycin (TOR) protein signaling in plants.  
662 *J Biol Chem* **287**(4): 2836-2842.

663 **Xiong Y, Sheen J. 2014.** The role of target of rapamycin signaling networks in plant growth and  
664 metabolism. *Plant Physiol* **164**(2): 499-512.

665 **Yu Y, Yoon SO, Poulogiannis G, Yang Q, Ma XM, Villen J, Kubica N, Hoffman GR, Cantley LC,**  
666 **Gygi SP, et al. 2011.** Phosphoproteomic analysis identifies Grb10 as an mTORC1 substrate that  
667 negatively regulates insulin signaling. *Science* **332**(6035): 1322-1326.

668 **Zhang Y, Persson S, Giavalisco P. 2013.** Differential regulation of carbon partitioning by the central  
669 growth regulator target of rapamycin (TOR). *Mol Plant* **6**(6): 1731-1733.

670 **Zhang YJ, Duan Y, Zheng XF. 2011.** Targeting the mTOR kinase domain: the second generation of  
671 mTOR inhibitors. *Drug Discov Today* **16**(7-8): 325-331.

672

673

674 Tables

675 Table 1: TOR targets identified with fold change values for drug condition versus control.

Accession	Common Name	Sites	Fold-change		
			AZD8055	Torin1	Rapamycin
<b>CrTORC1 proteins</b>					
Cre09.g400553.t1.1	TOR	S2598	0.99	0.90	1.12
Cre08.g371957.t1.1	RAPTOR	S782/S783:NL	1.56	1.94	1.54
<b>homologs of known substrates</b>					
Cre13.g579200.t1.2	RPS6KB	T771/S773/T777:NL	1.17	1.35	1.05
Cre09.g400650.t1.2	RPS6	T127	0.90	0.48**	0.61*
<b>homologs of TOR pathway-associated proteins</b>					
Cre10.g441200.t1.2	LARP1	T668/S670:NL	1.50	1.91*	1.96*
		S737/738:NL	0.08**	0.01**	0.99
		T809/S810:NL	0.41	0.46	0.81
		S817	0.06**	0.05**	0.13**
Cre17.g721850.t1.2	EEF2K	S306	0.75	0.42**	0.58
		S589/S591:NL	1.13	1.24	1.20
		S853/S857	2.00*	2.73**	1.69
Cre12.g516200.t1.2	EEF2	T57/T59:NL	4.75*	1.88	2.76
Cre12.g511850.t1.2	GSK3B	S322	1.27	1.15	1.25*
Cre09.g391245.t1.1	ATG1	T802/S803:NL	1.80	1.65	1.53
Cre06.g251050.t1.1	PRKAA	S699/S702:NL	0.64	0.29	0.97
Cre10.g457500.t1.1	PRKAB	S25/S29:NL	1.67*	1.75	2.27**
Cre02.g100300.t1.1	PI-3K/PI-4-like	T149/S150:NL	1.11	0.82	0.92
Cre05.g245550.t1.1	PI3KA	S794	1.04	0.91	1.51
Cre06.g304650.t1.1	PI3KB2	S403	1.25	1.39	0.88
Cre03.g192000.t1.2	SEH1	T478/S479/S482:NL	0.94	1.19	1.06
		S337	4.22	2.64	1.43
Cre02.g076900.t1.1	PRKG1	S71	2.20	1.54	1.59**
		S71/S78:NL	1.44	1.76*	1.41
		S126, S128	1.84	1.23	0.82
		T857/T859:NL	1.12	0.97	0.98
		T857/T859:NL	0.89	0.97	0.92
		T857/T859/T863:NL	1.45	1.17	1.22*
		S378	1.25	0.79	0.94
Cre10.g461050.t1.2	ATP synthase A	S378	1.25	0.79	0.94
Cre02.g076350.t1.2	ATP6B, ATPase	S7/S8:NL	2.24	1.12	2.09**
Cre11.g468550.t1.2	ATP synthase G2	S7	2.52*	1.62*	2.33
		S77	1.60	1.24	1.33

\*p-value  $\leq 0.05$  \*\*p-value  $\leq 0.01$

Up-  Down-

676

677 Fold change values shaded red indicate a statistically significant increase in phosphopeptide  
 678 abundance for specified drug treatment versus control. Fold change values shaded blue indicate a  
 679 statistically significant decrease in phosphopeptide abundance for specified drug treatment versus  
 680 control. Level of p-value statistical significance is denoted by p-value  $\leq 0.05$  (\*) and  $\leq 0.01$  (\*\*)

681 Table 2: Carotenoid content in WT Chlamydomonas after 8 hours of treatment with Rapamycin,  
682 Torin1, or AZD8055 compared to control.

683

### Carotenoids Content (mg g<sup>-1</sup> DW)

	Control	500nM Rap	500nM Torin	700nM Azd
Neoxanthin	0.64±0.01	1.12±0.01*	1.25±0.04*	1.65±0.00*
Violaxanthin	0.50±0.00	0.57±0.00	0.93±0.07*	1.02±0.00*
Anteraxanthin	0.04±0.00	0.12±0.00*	0.16±0.01*	0.11±0.00*
Lutein	1.60±0.03	2.56±0.02*	3.42±0.14*	3.29±0.00*
B-carotene	1.82±0.03	1.80±0.03	2.09±0.02*	3.02±0.02*



684 Figure Legends:

685 Figure 1. Drug treatment and cell harvesting workflow in *Chlamydomonas* cells. Replicate “n”  
686 (1-5) of each drug condition and control were harvested together prior to downstream processing.  
687 To minimize inter-condition batch effects, “n” replicate of each condition was harvested together  
688 and frozen until protein extraction.

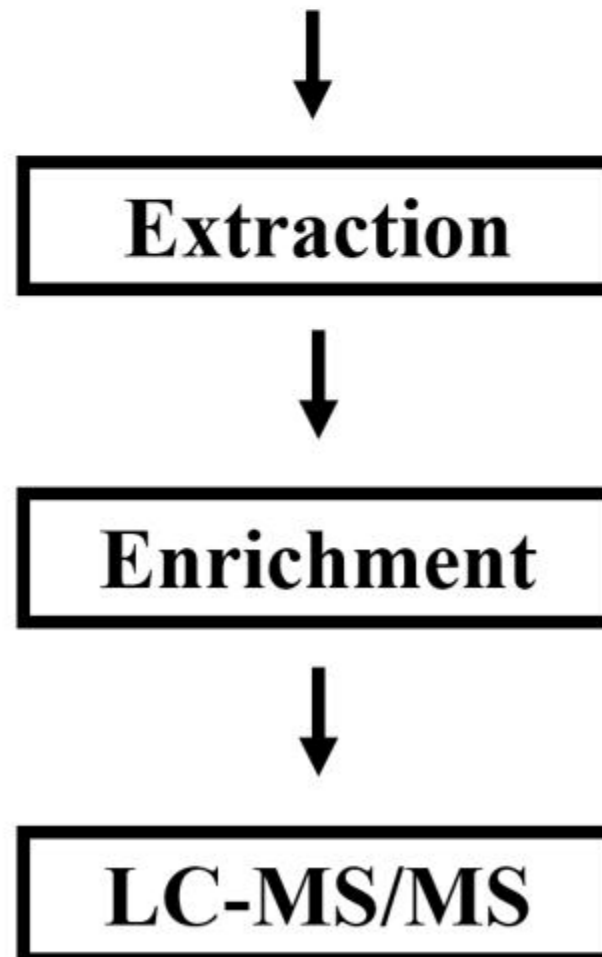
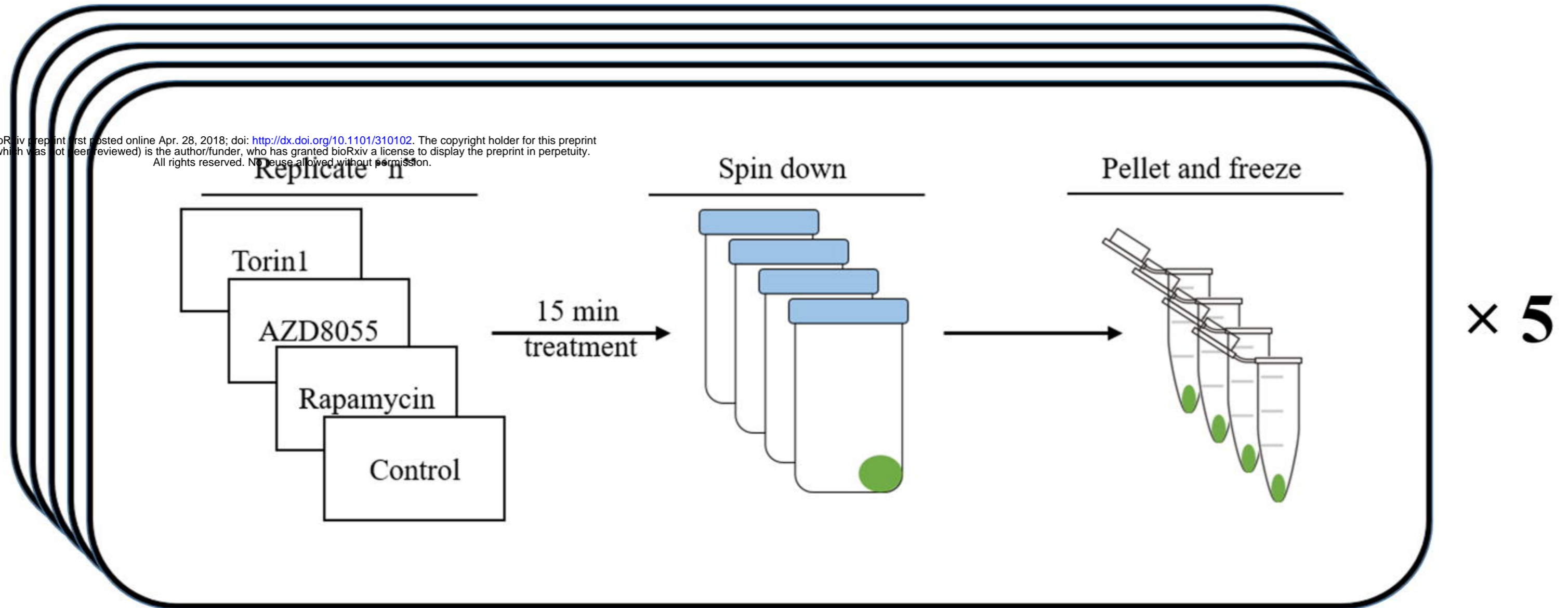
689 Figure 2: Sites modulated by TOR inhibition. Results of differential analysis between each  
690 chemical inhibitor drug treatment compared to control for both wild-type (a) and AZD-  
691 insensitive (b) *Chlamydomonas* strains. For comparison of overlap between the drug conditions  
692 in the WT dataset, a Pearson’s correlation was performed comparing all condition types. From  
693 this, the highest correlation among conditions was between AZD8055 and Torin1 at 0.986 and  
694 the lowest 3 were all drug inhibitor vs. controls.

695 Figure 3. Hierarchical clustering of differentially changing sites into 2 clusters (a). Visualization  
696 was performed in Perseus v1.6.0.0. Following data normalization and missing value imputation,  
697 intensity values were z-score normalized and grouped using k-means clustering with default  
698 parameters. Overall trends in site intensity were graphed and colored based on intensity (b). For  
699 each of the two clusters, motif analysis was performed (c). Sequence logo visualizations were  
700 performed using pLOGO with serine or threonine residues fixed at position 0. Positions with  
701 significant residue presence are depicted as amino acid letters sized above the red line. For  
702 cluster 1, there was significant enrichment for a proline in the +1 position and arginine in the -3  
703 position, RXXS/TP. For cluster 2, there was again significant enrichment for a proline in the +1  
704 position and arginine in the -3 position in addition to an aspartic acid in the +3 position,  
705 RXXS/TPXD.

706 Figure 4 Comparison of RPS6 protein sequence between *Arabidopsis* and *Chlamydomonas* (a). a  
707 western blot in wild-type under different drug treatments for 0, 5, 15, 30, and 60 min with  
708 antibodies raised for Ser242 (b).

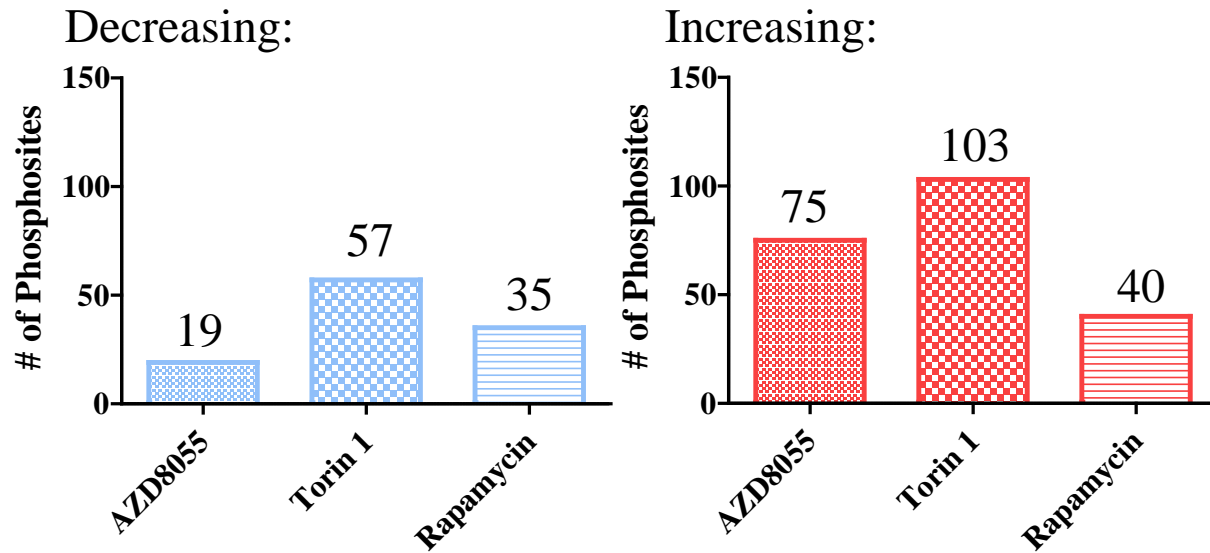
709 Figure 5: Bar charts of 10 modulated phosphosites on TOR pathway-associated proteins based  
710 on homology. Level of p-value statistical significance is denoted by p-value  $\leq 0.05$  (\*) and  $\leq$   
711 0.01 (\*\*)

712 Figure 6: Bar chart of carotenoid content in WT Chlamydomonas after 8 hours of treatment with  
713 Rapamycin, Torin1, or AZD8055 compared to control



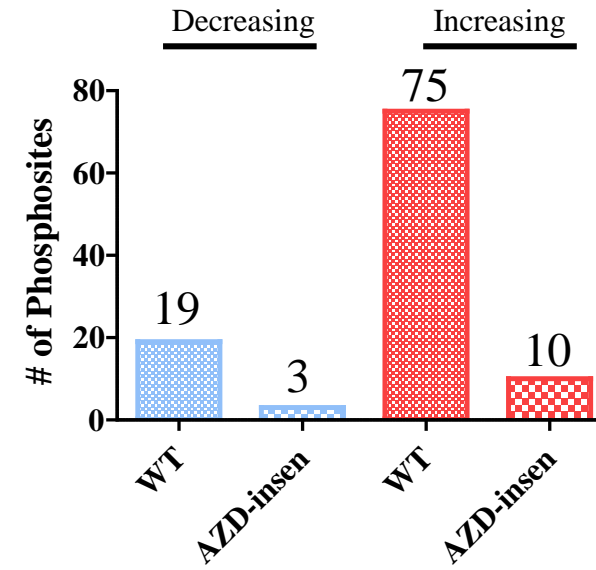
a.

**Wild Type**  
**258 phosphosites differentially changing**

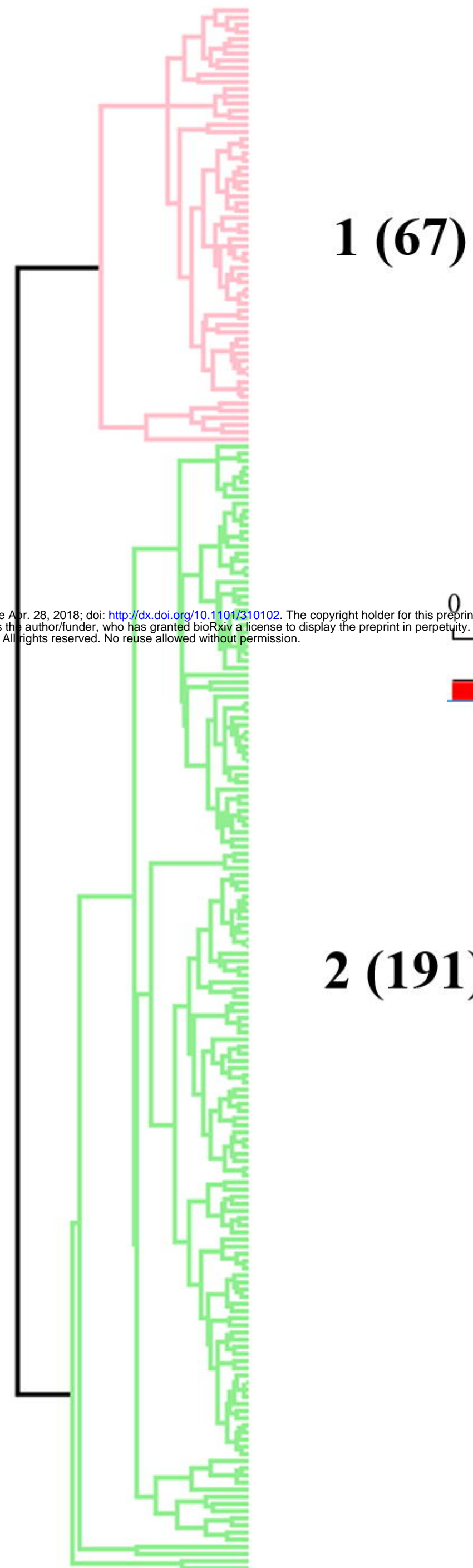


b.

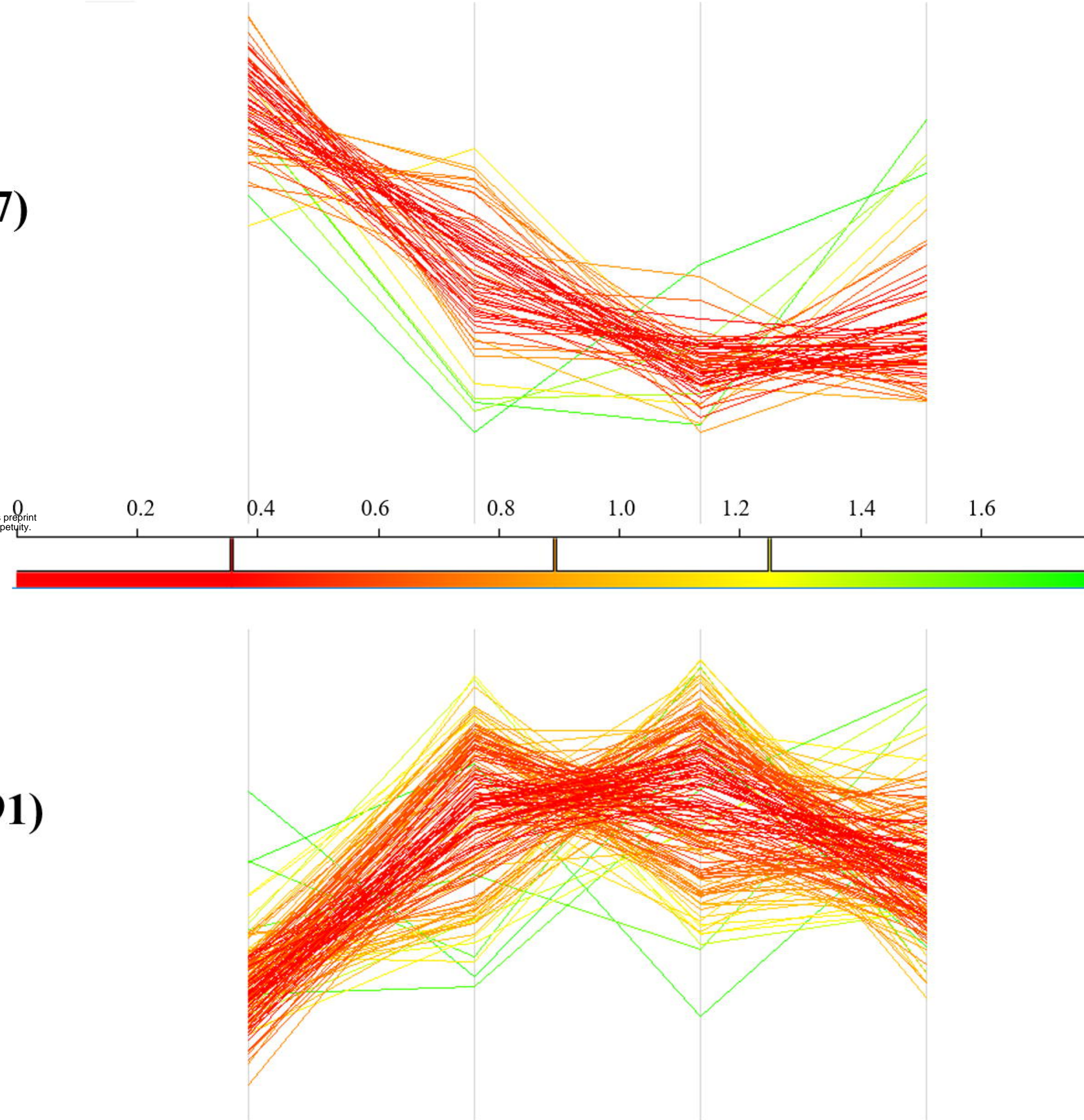
**AZD-insensitive**  
**13 phosphosites differentially changing**



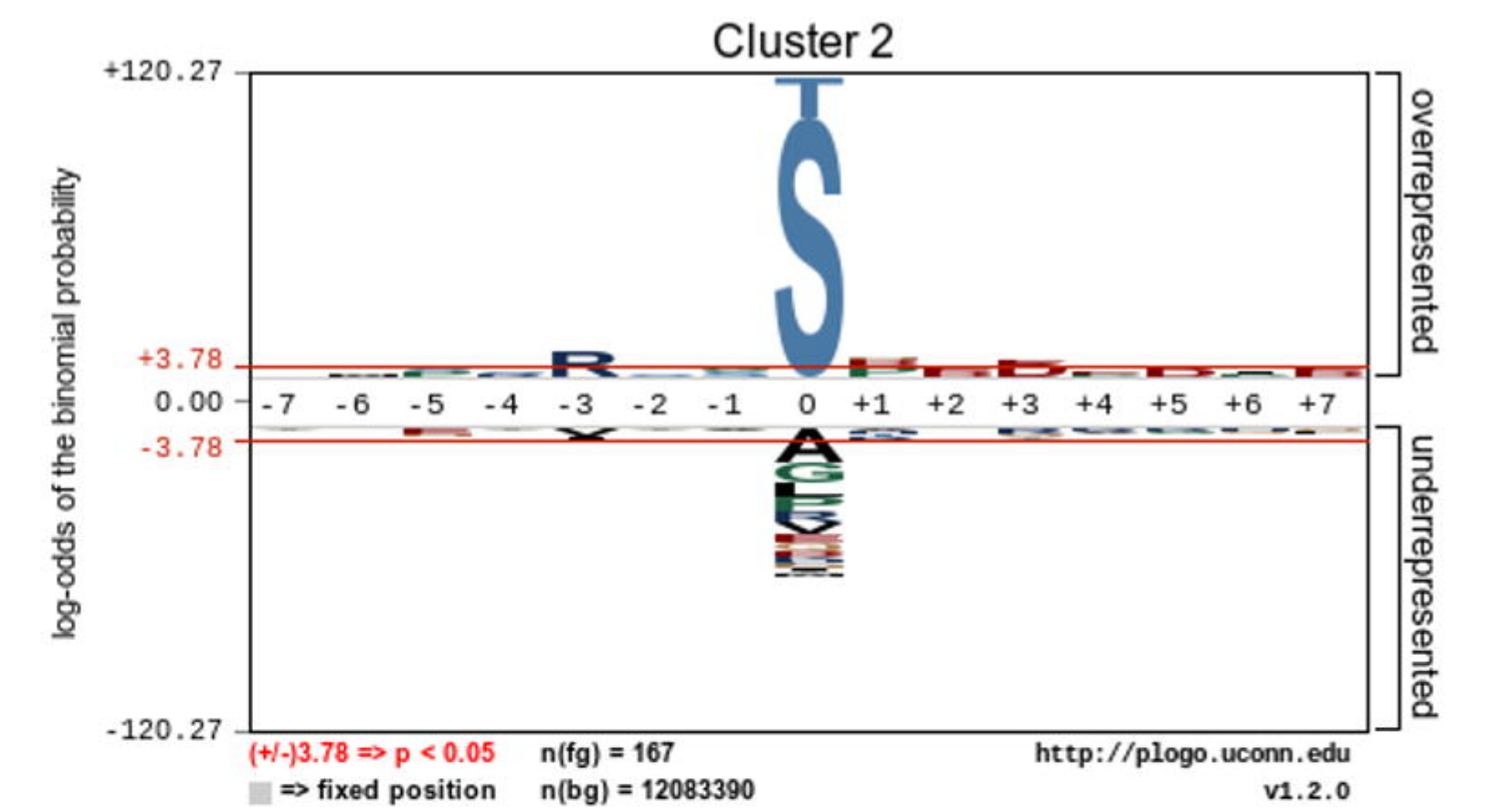
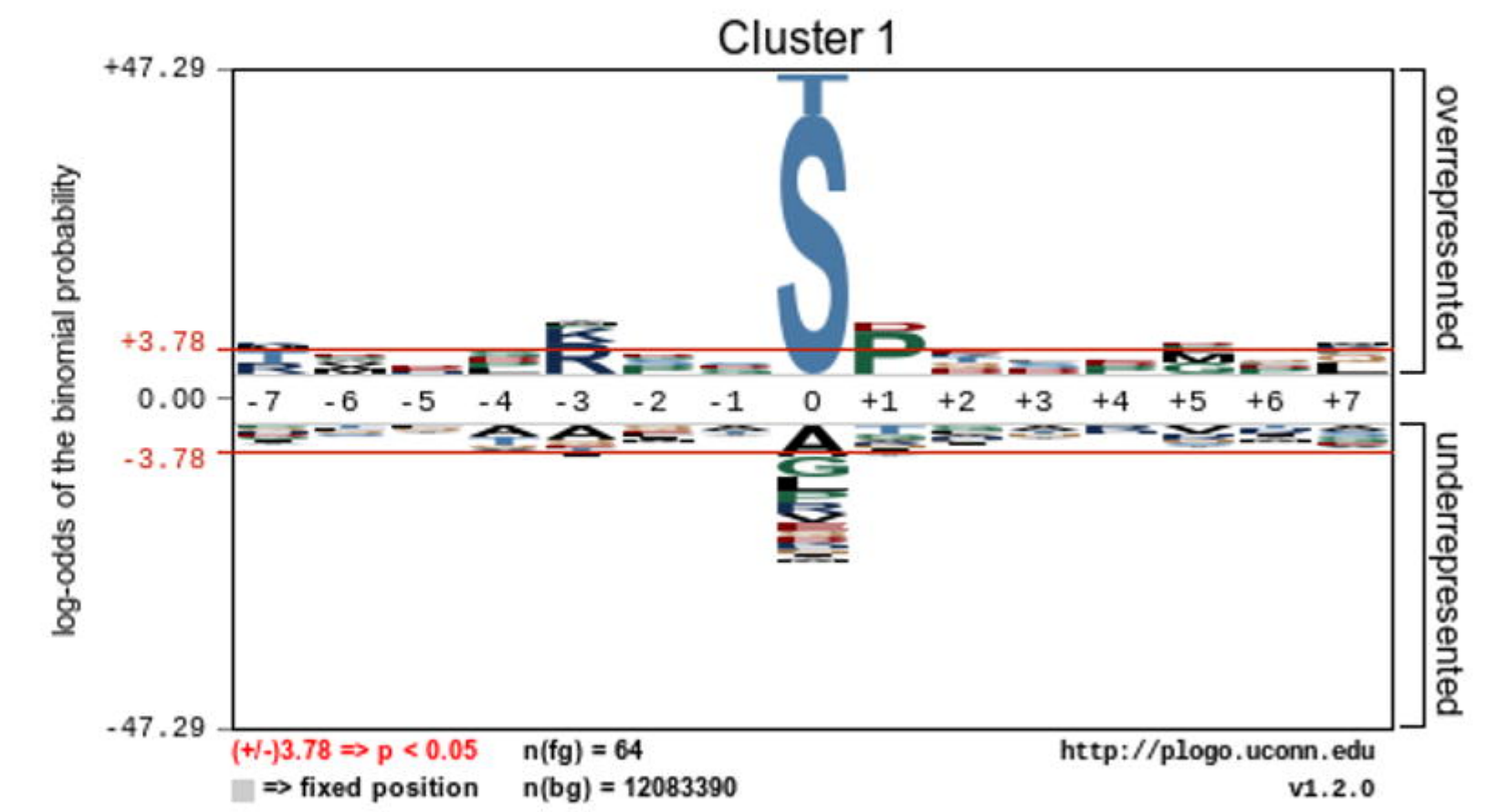
a. Cluster (# of phosphosites)



b. Control AZD8055 Torin 1 Rapamycin



c.

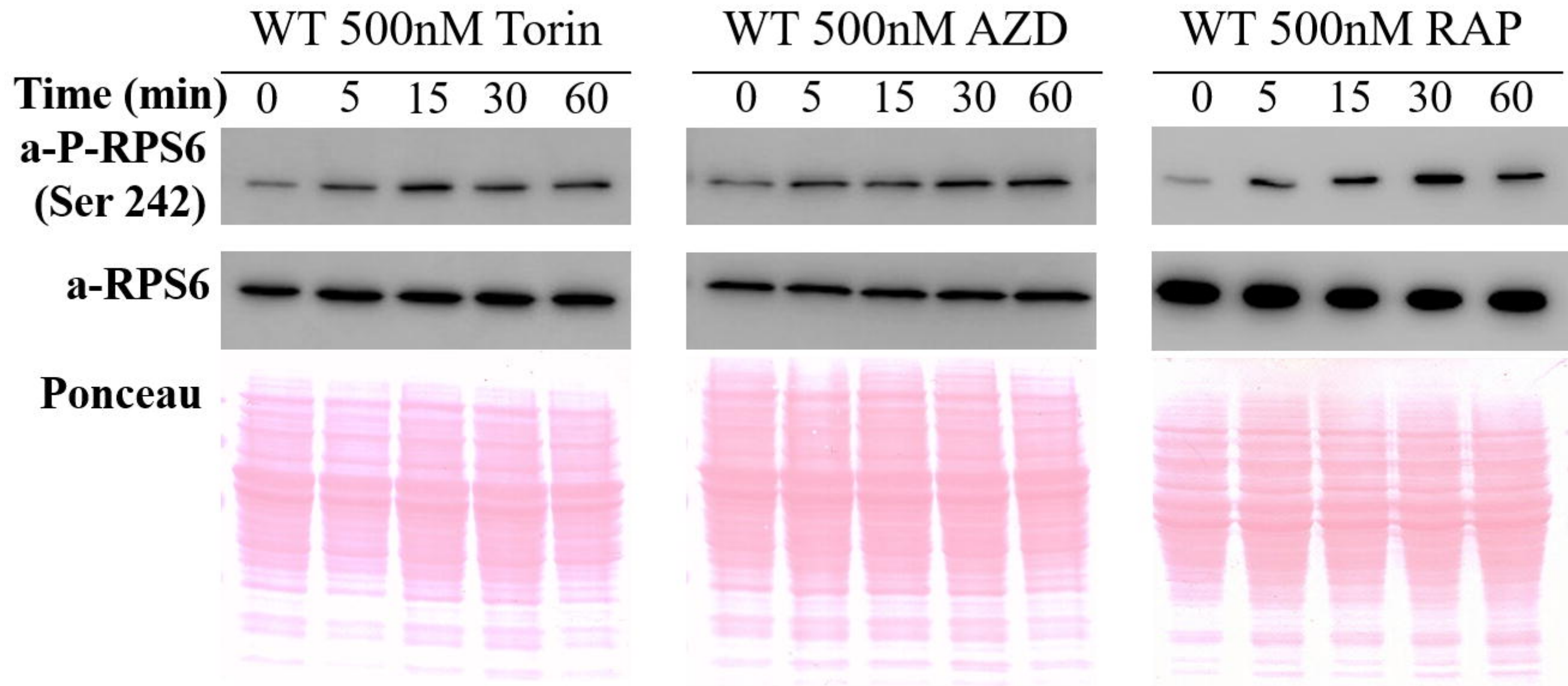


a.

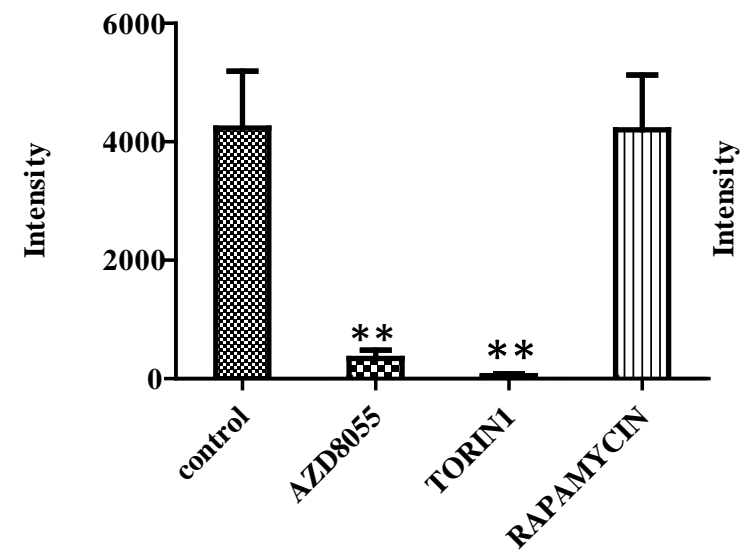
Score	Expect	Method	Identities	Positives	Gaps
316 bits(810)	1e-114	Compositional matrix adjust.	175/246(71%)	200/246(81%)	1/246(0%)
At RPS6	1	MKFNVANPTTGCQKKLEIDDDQKLRAFFDKRLSQEVSGDALGEEFKGYVFKIMGGCDKQG	60		
Cr RPS6	1	MK N+A P TGCQKKLE+DD+ KLRAF+D+R++ EV G+ LGEEFKGYV KI GG DKQG	60		
At RPS6	61	MKLNIAYPATGCQKKLEVDDEAKLRAFYDRRVAAEVDGEEFKGYVVKIAGGQDKQG	120		
Cr RPS6	61	FPMKQGVLTGRRVRLLLHRGTPCFRGGHRRRTGERRRKSVRGCIIVSPDLVNLVIVKKG	120		
At RPS6	121	F MKQGVLT RVRL+ G FRG+GRR GERRRKSVRGCIIVSPDL+VNLVIVKKG	180		
Cr RPS6	121	FAMKQGVLTNARVRLMTPGDQGFRTGRRRKSVRGCIIVSPDLAVNLVIVKKG	180		
At RPS6	181	SDLPGLTDEKPRMRGPKRASKIRKLFNLGKEDDVRKYVNTYRRTFTNKKGKKVSKAPKI	239		
Cr RPS6	181	+LPGLTD EKPR+RGPKRASKIRK+FNLGK DDVRKYV Y R T+K GKK K PKI	240		
At RPS6	240	QRLVTP LQQRKRIADKKKRIAKANSDAADYQKLLASRLKEQRDRRSESLAKKRS-RL	245		
Cr RPS6	241	QRLVTP LQQRKRIADKKKRIAKANSDAADYQKLLASRLKEQRDRRSESLAKKRS-RL	246		
At RPS6	240	SSAPAK	245		
Cr RPS6	241	ASQASK	246		

bioRxiv preprint first posted online Apr. 28, 2018; doi: <http://dx.doi.org/10.1101/310102>. The copyright holder for this preprint (which was not peer-reviewed) is the author/funder, who has granted bioRxiv a license to display the preprint in perpetuity. All rights reserved. No reuse allowed without permission.

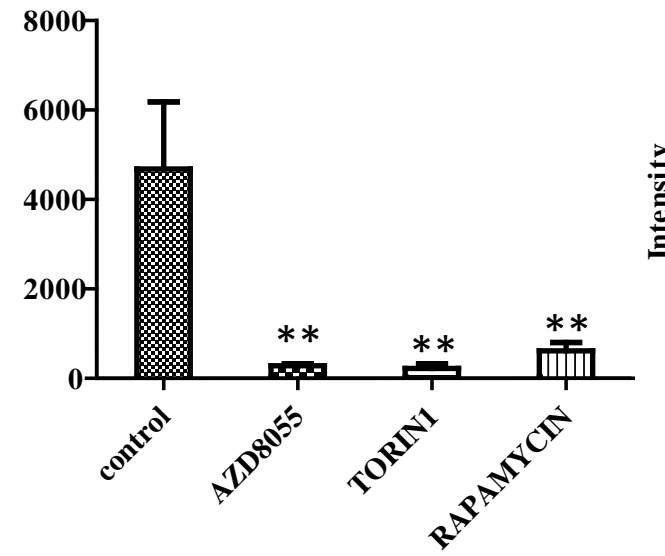
b.



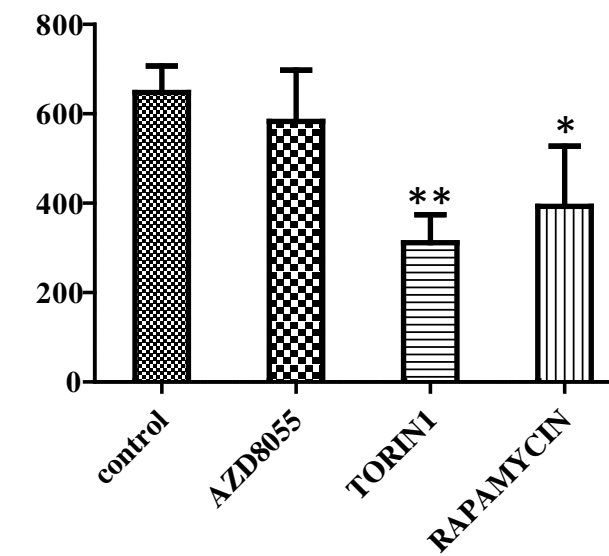
**Cre10.G441200.T1.2--S737/738:NL**  
**LARP1**



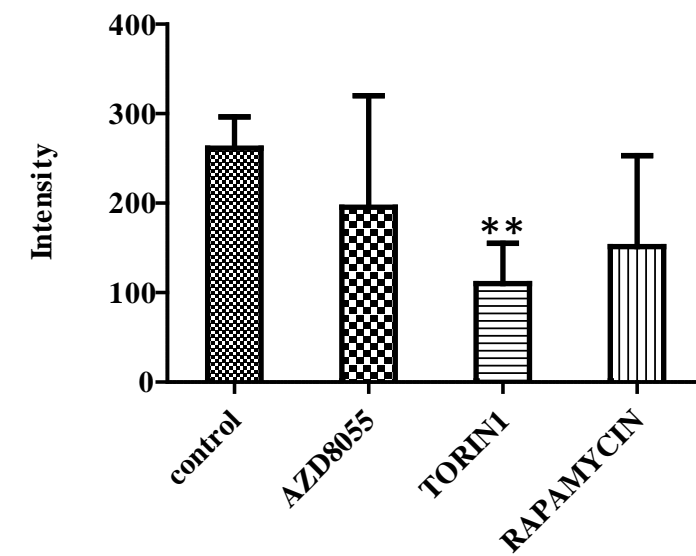
**Cre10.G441200.T1.2--S817**  
**LARP1**



**Cre09.g400650.t1.2--T127**  
**RP-S6e, RPS6**

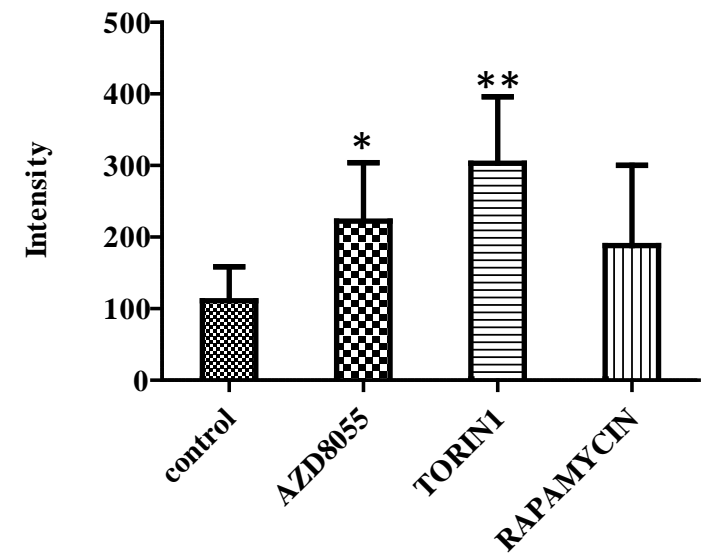


**Cre17.g721850.t1.2--S306**  
**EEF2K**

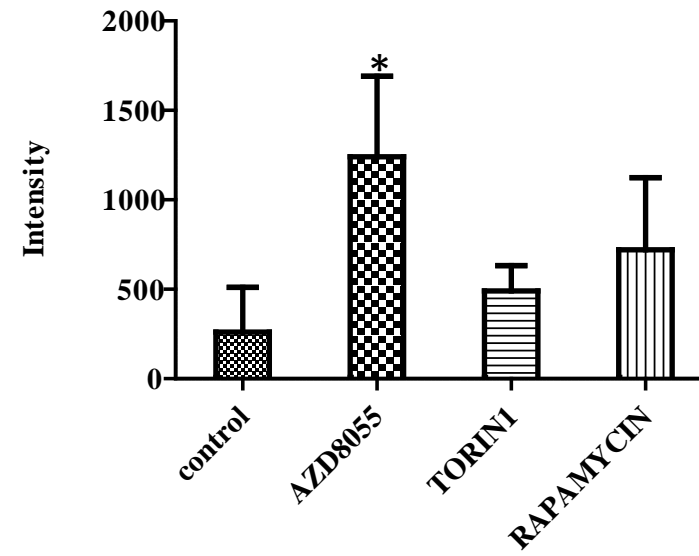


Decrease in phosphorylation

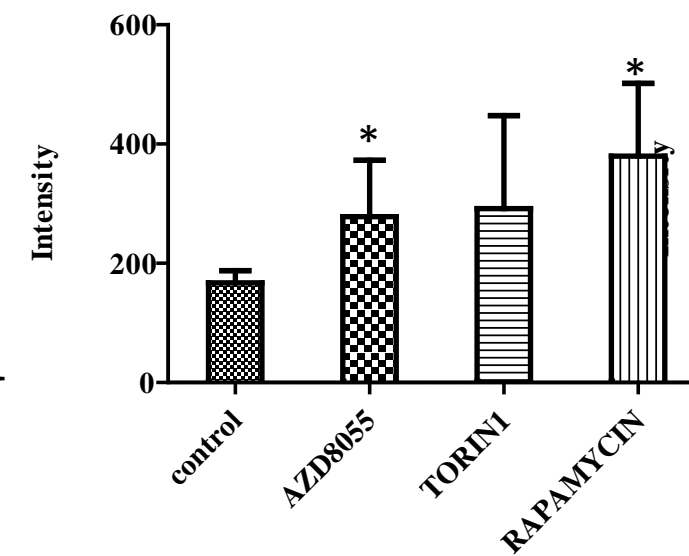
**Cre17.g721850.t1.2--S853/S857:NL**  
**EEF2K**



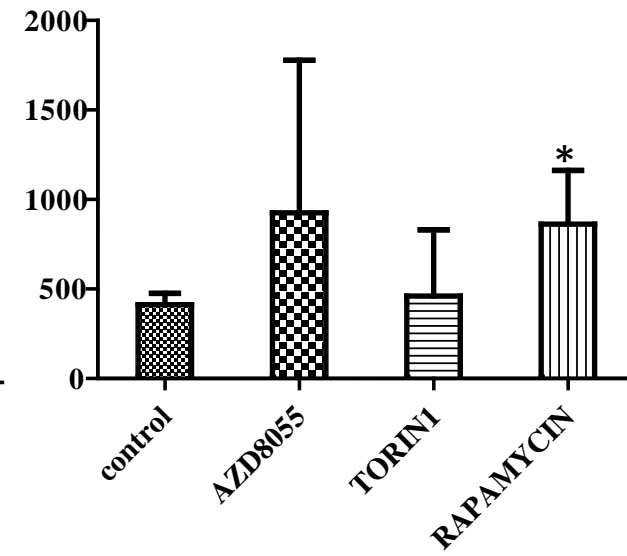
**Cre12.g516200.t1.2--T57/T59:NL**  
**EEF2**



**Cre10.g457500.t1.1--S25/S29:NL**  
**PRKAB**

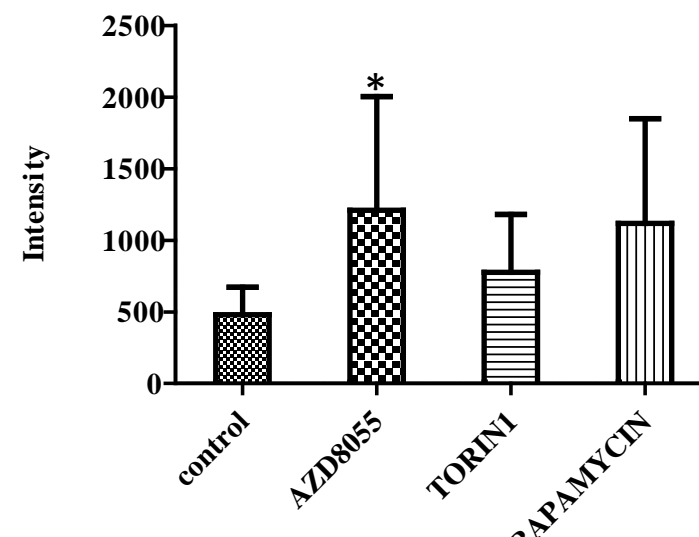


**Cre02.g076350.t1.2--S8**  
**ATP6B**



Increase in phosphorylation

**Cre11.g468550.t1.2--S7/S8:NL**  
**ATP6G**



**Cre02.g076900.t1.1--S71**  
**PRKG1**

